The Effect of Rotation Speed and Dwell Time on the Mechanical Properties and Microstructure of Dissimilar Aluminum-Titanium Alloys by FSSW Process

Mustafa Ali A. Glaissa

Submitted to the
Institute of Graduate Studies and Research
in partial fulfillment of the requirements for the degree of

Master of Science
in
Mechanical Engineering

Eastern Mediterranean University
January 2019
Gazimağusa, North Cyprus

Approval of the Institute of Graduate Studies and Research

Assoc. Prof. Dr. Ali Hakan Ulusoy
Acting Director

I certify that this thesis satisfies all the requirements as a thesis for the degree of Master of Science in Mechanical Engineering.

Assoc. Prof. Dr. Hasan Hacışevki
Chair, Department of Mechanical Engineering

We certify that we have read this thesis and that in our opinion it is fully adequate in scope and quality as a thesis for the degree of Master of Science in Mechanical Engineering.

Asst. Prof. Dr. Mohammed Bsher A. Asamel
Supervisor

Examining Committee

1. Assoc. Prof. Dr. Qasim Zeeshan

2. Asst. Prof. Dr. Mohammed Bsher A. Asamel

3. Asst. Prof. Dr. Amir Mirlatifi

ABSTRACT

Friction Stir Spot Welding (FSSW) is a novel solid-state joining process developed by Mazda and Kawaski and patented in 2003. It utilizes a profiled rotating pin that plunges into the joint and penetrates the material surface to the tool's shoulder and material is softened by heat-input generated by friction on contact area. FSSW has several advantages over fusion joining processes, as it is could be more cost-effective, durable and reliable than conventional spot welding processes. In addition, joints made by FSSW process have high shear tensile strength without adding weight than rivets, bolts, nuts and fasteners. Recently, many researches have applied FSSW for joining of similar as well as dissimilar alloys such as; Al-Al, Mg-Mg, Al-Cu, and Al-Mg alloys. This study focuses on FSSW of aluminum alloy with grade 5 titanium (AA 6061; Ti-6Al-4V), and the relationship between the welding parameters of; tool rotation speed and dwell time on the mechanical properties and microstructure of welded joint, which it is investigated by empirical observation utilizing SEM-EDS analysis, shear tensile and Vickers hardness tests. Tow-level factorial design was conducted for welding parameters. It is observed that the joint quality, mechanical behavior and microstructural evolution in the welded regions are considerably affected by the welding parameters. The microhardness profiles of titanium have significantly affected by heat-input. Additionally, maximum shear load was produced at 1000 rpm and 10 sec dwell time. SEM-EDS analyses detected the formation of Intermetallic Compounds (IMC) of $AlTi_3$ patterns near to Thermomechancial Affected Zone (TMAZ).

Keywords: Friction Stir Spot Welding, Aluminum Alloy, Titanium Alloy, Lap-joint, Welding Parameters

ÖZ

Sürtünme Karıştırma Nokta Kaynağı (FSSW), Mazda ve Kawaski tarafından geliştirilen ve 2003 yılında patenti alınmış yeni bir katı hal birleştirme işlemidir. Ekleme içine giren ve malzeme yüzeyini aletin omzuna geçiren profilli bir döner pim kullanır ve malzeme tarafından yumuşatılır. Temas alanındaki sürtünme sonucu oluşan ısı girişi. FSSW, füzyon birleştirme işlemlerine kıyasla, avantajlı nokta kaynak işlemlerinden daha uygun maliyetli, dayanıklı ve güvenilir olabileceğinden, çeşitli avantajlara sahiptir. Ek olarak, FSSW işlemiyle yapılan bağlantıların perçin, cıvata ve somun tutturuculara göre ağırlık eklemeden daha yüksek kesme gerilme mukavemeti vardır. Son zamanlarda, pek çok araştırma, benzerlerinin yanı sıra benzer olmayan alaşımların bir araya getirilmesi için FSSW'yi uygulamıştır; Al-Al, Mg-Mg, Al-Cu ve Al-Mg alaşımları. Bu çalışma 5. sınıf titanyumlu (AA 6061; Ti-6Al-4V) alüminyum alaşımlı FSSW ve kaynak parametreleri; Kaynaklı mafsalın mekanik ve mikroyapısal özellikleri üzerinde takım dönme hızı ve durma süresi, SEM-EDS analizi, kesme gerilmesi ve Vickers sertlik testleri ile ampirik gözlemlerle incelenmiştir. Kaynaklı bölgelerdeki eklem kalitesi, mekanik davranış ve mikroyapısal evrimin kaynak parametrelerinden önemli ölçüde etkilendiği görülmektedir. Titanyumun mikro sertlik profilleri, ısı girişinden önemli ölçüde etkilenmiştir. Ek olarak, maksimum devir sayısı 1000 rpm'de ve 10 saniye kalma süresinde üretildi. SEM-EDS analizleri, Thermomechancial Affected Zone (TMAZ) 'a yakın $AlTi_3$ desenlerinin İntmetalik Bileşiklerinin (IMC) oluşumunu göstermiştir.

Anahtar Kelimeler: Sürtünme Karıştırma Nokta Kaynağı, Alüminyum Alaşımı, Titanyum Alaşımı, Lap-eklem, Kaynak Parametreleri

DEDICATION

To My Family.

ACKNOWLEDGMENT

I would first like to thank my thesis advisor Asst. Prof. Dr. Mohammed Asamel of the mechanical engineering department at Eastern Mediterranean University (EMU). He consistently allowed this thesis to be my own work, but steered me in the right direction whenever he thought I needed it.

I would also like to thank Assoc. Prof. Dr. Qasim Zeeshan whose office was always open whenever I ran into a trouble spot or had a question about my research or writing.

Finally, I would like to acknowledge the department of metallurgical and materials engineering at Middle East Technical University (METU) for their great contribution to this work and pleasant hospitality.

TABLE OF CONTENTS

LIST OF TABLES

LIST OF FIGURES

LIST OF ABBREVIATIONS

AA	Aluminum Alloy
BM	Base Metal
DT	Dwell Time
EDS	Energy-dispersive X-ray Spectroscopy
FSSW	Friction Stir Spot Welding
FSSWed	Friction Stir Spot Welded
FSWed	Friction Stir Welded
HAZ	Heat Affected Zone
HV	Vickers Hardness
IMC	Inter Metallic Compound
RPM	Revolution Per Minute
SEM	Scanning Electron Microscope
SZ	Stir Zone
TMAZ	Thermo Mechanical Affect

Chapter 1

INTRODUCTION

1.1 Background

Friction Stir Spot Welding (FSSW) process was derivative of Friction Stir Welding (FSW) process. This method was developed by Mazda and Kawasaki in 2003, which it was used to join the structure of Mazda Rx-8 rear seats (Pan 2007). This solid state process is able join metals without reaching to melting point. The principle of this process is based on the usage of a profiled rotating pin under certain vertical load to penetrate the surface of workpiece to be joined; and then the pin gradually starts plunging into the joint surface to penetrate and soften materials due to applied stir friction on surface by tool's shoulder at a specific dwell time. This mechanism is schematically illustrated in Figure 1. This process induces sufficient heat to join parts without causing sever distortion in weld joints (Mubiayi et al. 2018). However, the use of FSSW process has significantly expanded in different industrial sectors such as; automotive, railways, and aerospace. Process is characterized by the ability of joining dissimilar metals that cannot be welded by fusion process and it gives great mechanical properties, wide range of joint geometries and less distorted joints. Furthermore, FSSW process uses various types of tools made from metal alloys and heat treated ceramic that can retain high strength at elevated temperatures (Grimm et al. 2015). FSSW shares the main welding principle with FSW method. Additionally, this process can be automated to join metal panels in automobile sector as illustrated in Figure 2 (Wang et al. 2018). However, FSSW is can be done only vertical-linear

motion, such as welding of roof panel and the Al train body shown in Figure 3 and 4 respectively (Yamaguchi. 2004), **(**Tozaki et al. 2009).

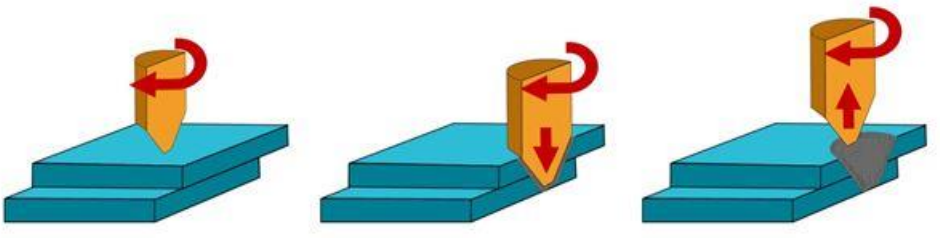

Figure 1: Principle of friction stir spot welding process

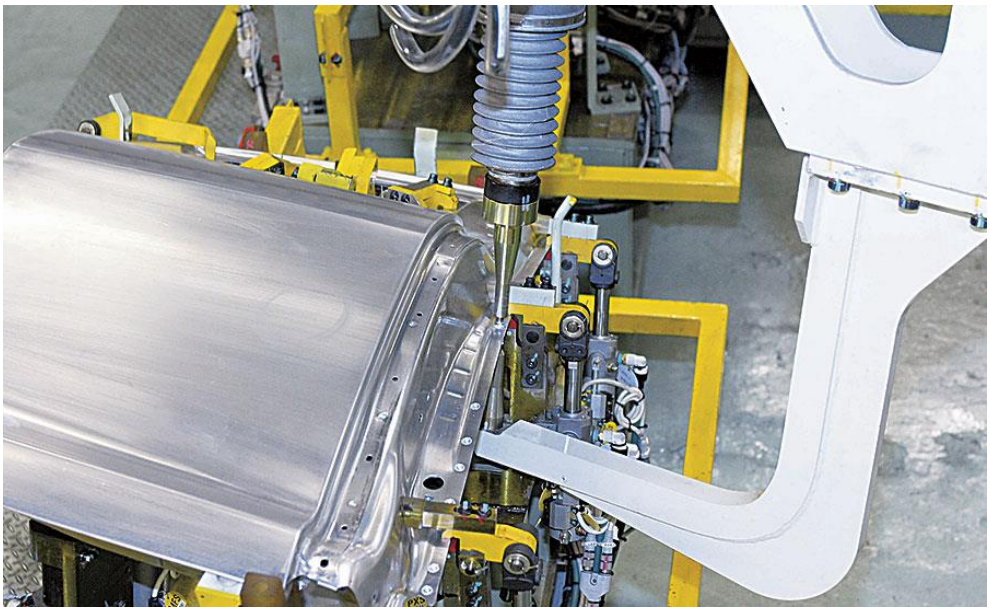

Figure 2: FSSW of rear doors at Mazda motor cop factory (Wang et al. 2018)

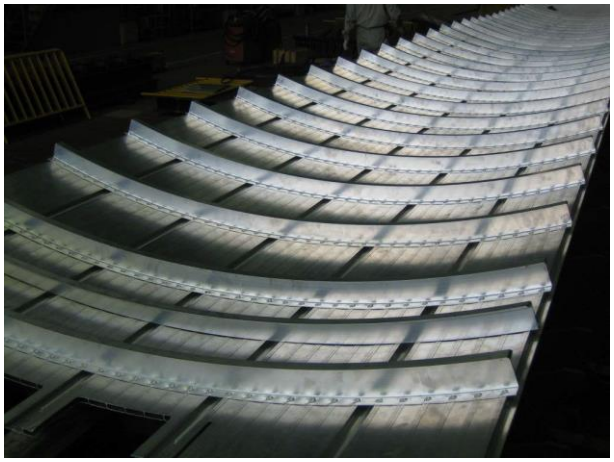

Figure 3: FSSW of roof panel (Yamaguchi 2004)

Figure 4: FSSW prototype (Tozaki et al. 2009)

Titanium alloys are widely used in aeronautical and aerospace sectors, because of their high strength to weight ratio, excellent corrosion resistance and low thermal conductivity. Super alloys such as titanium, have swept over the major share in the aerospace industry as shown in Figure 5 (Islam and Rahman 2014). The most used titanium alloy in aerospace industry is Ti-6Al-4V which is classified as G5 titanium, due its great machinability feature that used i.e. in designing fans of the inlet side of airplanes engines for temperatures up to 300 °C and also it is designed for making airframes, bolts, and seat railways (Inagaki et al. 2014).

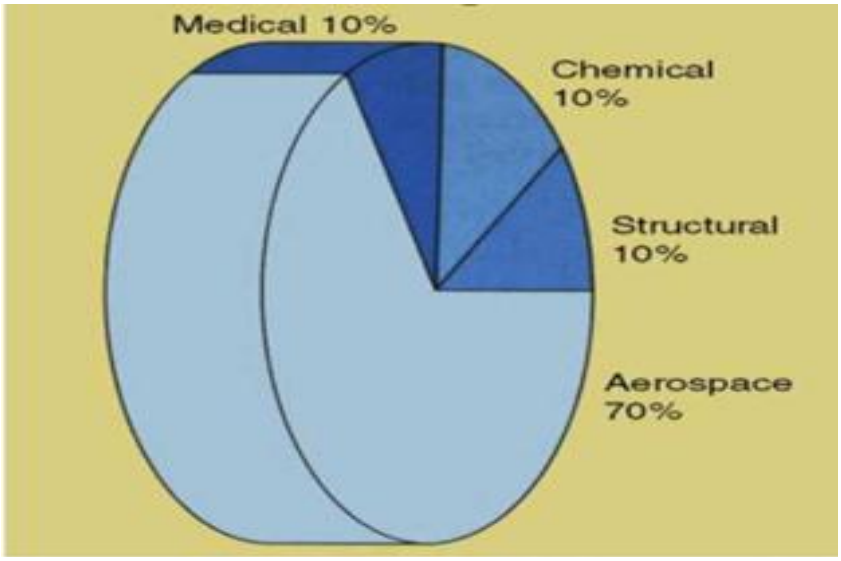

Figure 5: Titanium share among various industries (Islam and Rahman 2014)

High market demands in terms of low cost, low fuel consumption and high strength car bodies, makes aluminum a strong candidate in the field of automobile industry. The density of aluminum is about one-third of the steel with high stiffness.Thus, it considers as an engineering potential solution to meet these requirements as it has been suggested by the original equipment manufacturer (OEM) (Tisza and Czinege 2018). Recent researches have focused on reducing the structure body weight by selecting the proper aluminum alloy for the body-in-white (BIW) process, where it is expected that weight reduction ratio up to 40% from the car total weight (Budai et al. 2017). Significant improvements have been done on aluminum alloys since they were first introduced in the 1920s. That is to say, the deep understanding of aluminum chemical compositions, heat treatments, and controlling of impurity are the main concerns to these improvements (Rambabu et al. 2017). In terms of aerospace industry, aluminum alloys play a major rule in fabricating different airplanes parts. In long-haul international flights of jumbo jets, imposed that engine parts and shell must be highly durable and fatigue- resistance. Therefore, plenty of aluminum alloys types are developed over the years. For example, AA 6061 is a used

in light aircraft; mostly the homemade ones. It is without difficulty welded & manipulated, very light and properly strong, making it perfect for fuselage and wings (Danylenko. 2018).

1.2 Problem Statement

Achieving high quality and defect-free welded joints which lead to reduce mechanical properties are the main goals for the most of solid and fusion state welding process. Nevertheless, the drop in joint strength remains an issue that has to be solved for similar and dissimilar parts to be welded. Fusion welding of titanium alloys is challenging and causes root defects in weld joints, because of to the low thermal conductivity. In addition, complexity of joining aluminum to titanium alloys by means of fusion welding due to the large difference in their melting point; 582 °C and 1878 °C respectively. However, these issues can be overcome by utilizing solid-state welding such as FSW or FSSW processes (Ramirez and Juhas. 2003).

As a variant of friction stir welding process, FSSW has been proposed to produce spot welds. It shows great potential to replace of single-point joining processes similar to resistance spot welding (RSW) and riveting. It has wider applications in aerospace and aviation fields. For this purpose, the correct joining process at optimized parameters must be taken into account during welding. Additionally, FSSW is used recently to weld car hood and rear seats made from aluminum panels (Yang et al. 2014).

To understand how the material flows during different stages of FSSW. It is practically important and essential to achieve the optimized welding parameters for obtaining high efficiency welds. In some literature material flow has been reported as

one of the significant factors that affect welding quality which need to be optimized and controlled such as the rotation speed and dwell time (Yuan 2008).

In case of joining dissimilar metals titanium to aluminum (Ti-Al) lap-joint; intermetallic compound (IMC), .i.e., Al_3Ti is formed within the welding zones. This IMC causes brittleness and microcracks in weld joint (Fujii et al. 1994; Chen et al. 2011; Shouzheng et al. 2014). In order to overcome the formation of Al_3Ti phase researchers have reported that joining aluminum to titanium will restricte the formation of Al_3Ti and increase the tensile ductility of the welded joint. Additionally, joining of Al-Ti lap-joint utilizing FSSW process is challenging due to the possibility of initiating microcracks near stir zone (SZ) periphery at high rotation speed. Formation of intermetallics; AlTi and $AlTi_3$ within the cross-section of FSSWed workpiece are also expected (Chen et al. 2011).

1.3 Objectives of the Study

i. To achieve full adhesive FSSWed lap-joint of AA 6061 with Ti-6Al-4V alloys.
ii. To investigate the effect of welding parameters on the quality and mechanical properties of FSSWed joint.
iii. To investigate the effect of welding parameters on the formation of intermetallic compounds in the TMAZ or HAZ of FSSWed joint.

1.4 Scope of the Study

i. The aluminum-titanium (AA6061 and Ti-6Al-4V) plates with 4 mm in thickness will be lap-joined together by utilizing FSSW process.

ii. Utilizing metallurgical microscope and SEM-EDS analysis will contribute to detect weld defects, fracture regions, un-welded areas and emerged intermetallic compounds.

iii. Applying mechanical tests of shear tensile and Vickers hardness test in order to investigate the mechanical properties of Al-Ti lap-joint.

1.5 Organization of the Thesis

This work consists of five chapters. The first chapter is introduction, that includes background, problem statement, objective of the study, scope of the study and as well as organization of the thesis. Additionally, to the Introduction, a literature review is presented within Chapter 2, displaying a description of aluminum and titanium alloys, with a focus on classifications of titanium alloys;1)alpha and near alpha 2) alpha and beta, 3) beta & near beta. Application of titanium alloys in aerospace and automotive sectors are presented respectively. Moreover, aluminum & aluminum alloys classification and their applications are discussed in details. Types of welding methods such as; 1) laser beam welding (LBW), 2) gas metal arc welding (GMAW) of titanium, 3) gas tungsten arc welding (GTAW), 4) resistance spot welding (RSW), 5) friction stir spot welding (FSSW) process overview. Recent researches on FSSW are also presented at the end of chapter 2, the gaps and key findings of the literature review are discussed.

Chapter 3 presents the methodology of this study; including, materials preparation, experimental setup, FSSW tool, DOE, welding procedure, mechanical tests and metallographic inspection are clearly explained.

Chapter 4 shows the results for each of mechanical and metallographic investigations separately and provides a discussion for each with comparison to previous studies; aiming to validate data results established. Chapter 5 presents the conclusion and future recommendations of this study.

Chapter 2

LITERATURE REVIEW

2.1 Introduction

This chapter focuses on the recent literature related to friction stir spot welding (FSSW). The factors affecting the friction stir spot welding process are outlined, in addition to any previous studies conducted on fusion and solid state welding of aluminum and titanium, as well as aluminum to other materials are also summarized.

2.2 Titanium and Titanium Alloys

Titanium and its alloys have been used extensively as industrial alloys for over 60 years, satisfying the requirement for materials with high energy-to-weight ratios at high temperatures, and they were used within the aerospace and defense industries. Over 80% of titanium produced is utilized in these industries, typically in the wrought form, however many different applications are limited because of their negative tribological properties and high extraction cost, which approximately five times that of steels and aluminum alloys (Baker 2010). In addition, an oxidation property for titanium is a major issue, due to its high affinity for atmospheric gases such as; oxygen, hydrogen and nitrogen that can be easily absorbed. Nitrogen can has the ability to embrittle titanium and reduces its elongation under sustain load as illustrated in Figure 6 .However, titanium alloys have great corrosion resistance to sea water due to the formation of protective oxide layer. Titanium is a non-magnetic and poor conductor metal that has a high melting-point of 1678 °C, which is 1000 °C

more than of aluminum, which shows that titanium alloys can handle creep resistance over a wide range of temperatures (Padmanabhan et al. 2001).

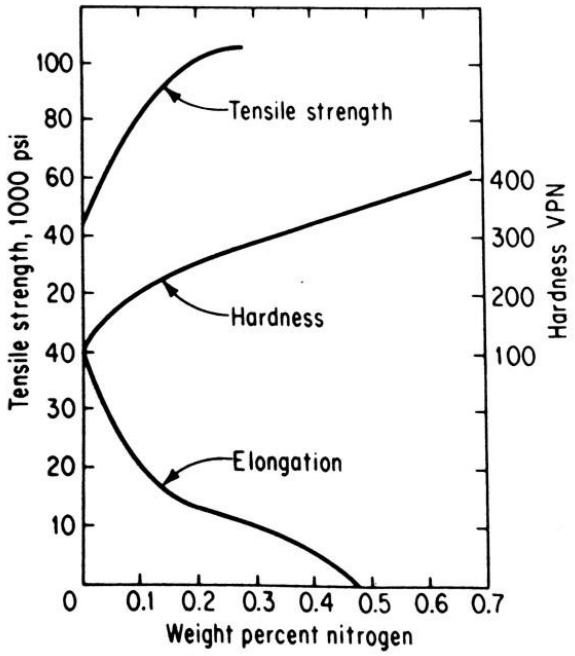

Figure 6: Effect of presence of nitrogen in pure titanium (Brick and Phillips 1949)

2.3 Classifications of Titanium Alloys

Commercially Pure titanium (CP Ti) has a high melting point 1670 °C and can resist corrosion at elevated temperature which is used in chemical process industries. However, it is rarely used in mechanical applications without alloying, due to its low strength in compare of most other titanium alloys. In recent years, using of titanium alloys have increased drastically because of the improvement of techniques concerned of their fabricating and further processing. Some classification of unalloyed titanium and titanium alloys are given in Table 1.

Table 1: Titanium Alloys (Peters 2003)

Unalloyed Ti-Grades	Alpha and Near Alpha	Alpha and Beta	Beta and Near Beta
ASTM GRADE	Ti-6%Al-2%Sn-	Ti-6%Al-2%Sn-	Ti-5%Al-2%Sn-

	4%Zr-2%Mo	4%Zr-6%Mo	2%Zr-4%Mo-4%Cr
ASTM GRADE-2	Ti-6%Al-3%Sn-4%Zr-0.5%Si	Ti-6%Al-4%V ELI	Ti-10%V2%Fe3%Al
ASTM GRADE-3	Ti-5%Al-4%Sn-4%Zr-1%Nb	Ti-6%Al-4%V	
ASTM GRADE-4	Ti-8%Al-1%Mo-1%V	Ti-6%Al-6%V-2%Sn	
ASTM GRADE-7	Ti-5%Al-2.5%Sn		
	Ti-5%Al-3%Sn-3%Zr-1%Nb		

2.3.1 Alpha and Near Alpha

This type is not heat treatable with α-phase and contains major alloy element of aluminum that improves the stabilization of alpha phase. Near alpha titanium alloy such as Ti3Al2.5 V is regularly used to production of seamless tubing for airplane hydraulic systems (Leyens and Peters 2003).

2.3.2 Alpha and Beta

These types of titanium alloys are heat treatable with risk of reducing some ductility of the metal and have poor creep strength comparing to near alpha alloy (Donachie. 2000). The titanium alloy Ti-6Al-4V (Grade 5) represents about 56% of US titanium market (Lütjering and Williams 2007). Figure 7 shows the phase diagram of Grade 5 titanium alloy. Thus, (HCP) crystal structure is denoting for α phase and (BCC) is denoting for β phase. Phase transition from α →β occurs at 4% of vanadium starting from 650 °C until reaching 1050 °C (Ducato et al. 2013).

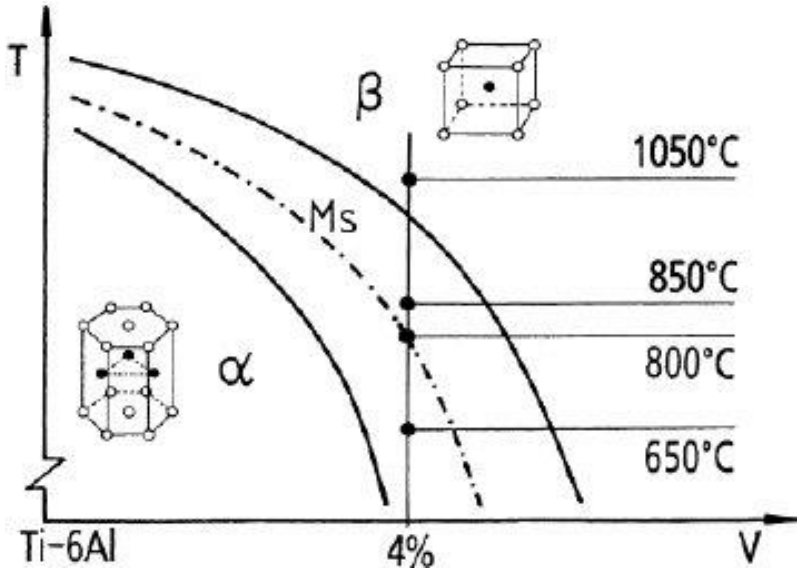

Figure 7: Ti-6Al-4V phase diagram (Ducato et al. 2013)

2.3.3 Beta and Near Beta

These alloys are heat treatable, mostly weldable and have high to intermediate strength at elevated temperatures (Donachie 2000). β type titanium alloys with poorer moduli of elasticity and better strength have been developed lately. Beta titanium alloys normally can be fabricated to greater strength levels and show better notch properties and toughness than α-β alloys (Wang 1996).

2.4 Applications of Titanium Alloys in Aerospace

In comparison to steels and aluminum alloys, titanium alloys need to be considered as much younger structural material. The primary alloys had been advanced on the end of the 1940s in the United States. Amongst these turned into the classic titanium alloy, Ti-6Al-4V, which still captures a massive part of aerospace industry nowadays (Leyens and Peters 2003). Due to the high corrosion resistance and excellent specific strength titanium alloys play a major role in the aerospace applications as:

- Reduction in weight (replacement for steels)
- Temperature applications (replacement for steels and Al alloys)
- Corrosion resistance (replacement for low-alloyed steels and Al alloys)

- Limitation of space (replacement for steels and Al alloys)

2.5 Applications of Titanium Alloys in Automotive

In recent years, titanium alloys have involved in the automotive industry especially in racing cars engines early in 1980s, duo to their high efficiency. The robust interest revealed in titanium materials by the industry in terms of lightweight, fuel-efficiency, and performances (Fujii et al. 2003). The design for body structure materials are based on aluminum and magnesium alloys duo to their high torsion and bending strength. On the other hand, the interior parts of engine such as connecting rods and intake valves as listed in Table 2 are made from various titanium alloys, due to their high yield strength (Leyens and Peters 2003). A number of car parts that are fabricated from titanium are shown in Figure. 8.

Table 2: Engine Parts Made From Titanium (Peters 2003)

Year	Component	Material	Manufacturer	Model	Annual consumption
1998	Brake	Grade 1s	Volkswagen	All	˜ 40 t/yr
1999	Connecting Rods	Ti-6Al-4V	Porsche	GT3	˜ 1 t/yr
1999	Valves	Ti-6Al-4V & PM-Ti	Toyota	Altezza	n/a
2000	Suspension Springs	LCB	Volkswagen	Lupo-FSI	3-4 t/yr
2001	Exhaust System	Grade 2	GM	Corvette Z06	>150 t/yr
2002	Valves	Ti-6Al-4V & PM-Ti	Nissan	Infinity Q 45	n/a

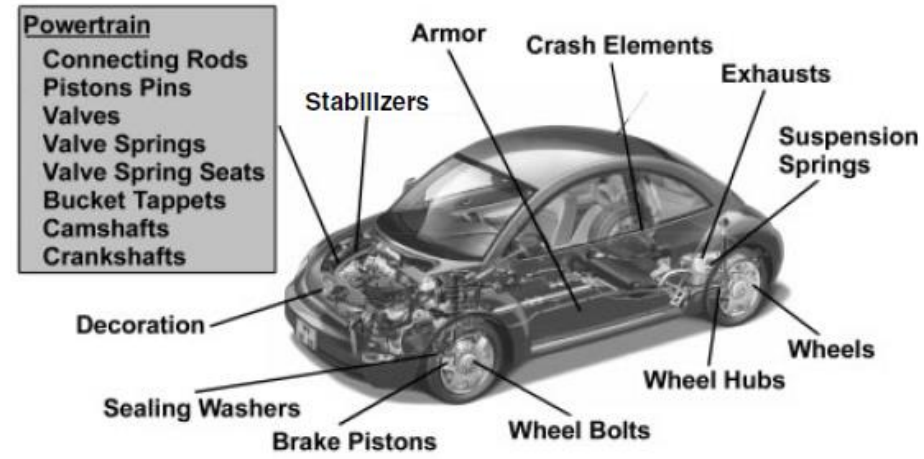

Figure 8: Titanium alloys parts in automobiles (Peters 2003)

2.6 Aluminum and Aluminum Alloys

Aluminum has unusual properties and different welding requirements, and it is used widely throughout the manufacturing industry. Aluminum is one of the few metals that aren't mined; it does not exist naturally like iron, gold or silver. Rather it is a product of bauxite which it can be found in almost every shovel full of earth throw-out the world. Through an electrolytic process (bauxite refined into alumina), and which is further refined into pure aluminum (Lumley 2010). Although, aluminum has a number of valuable properties, it is best known for its light weight and high strength. A single pound of aluminum is three-times larger than the same amount of steel. The tensile strength (TS) of aluminum is also very changeable, thus by cold working the metal, i.e., cold rolling, TS can be increased from 89.63 MPa to 179.26 MPa. TS can be increased even further 689.48 MPa by alloying, heat-treating, cold-working and aging. Metals commonly alloyed with aluminum are silicon, zinc, magnesium, copper and manganese, in addition, aluminum is durable; under most conditions parts made from aluminum will resist the destructive effects of corrosion unlike parts manufactured from steel or iron. A tough oxide coating (passive layer) forms quickly on the exposed surface of aluminum sealing of the air and protecting

the underline metal like self-repairing and self-limiting transpiring shield (Grushko et al. 2016).

2.6.1 Classifications of Aluminum Alloys

Aluminum is often alloyed with various metals to produce different properties especially suited for particular application, theses alloys use the aluminum association numbering system for identifying the various alloying elements and metals properties. The numbering system has been standardized, i.e., 4XXX, so that the first digit indicates the major alloying element, the second digit modifications to the original alloy such as heat treating or cold working and the last two digits identify the specific alloy content or degree of aluminum purity. There are eight major series of aluminum alloys as listed in Table 3 and they are given in a numerical designation according to the most important alloying metal in the mixture (Belov et al. 2014).

Since the aluminum can be manufactured in a variety of strengths, a standardized system of suffixes (O-F-H-T) are added to the end of the four digit classification to represent strength of the material. Where, O indicates an alloy in the annealed state, F as fabricated, but has not received any additional strengthening, H as strain hardened are non-heat treatable alloys and are strengthened by strain hardening or cold working and T suffix alloys are heat treatable in order to increase harness, .i.e., quenching process (Pearson 2013).

Table 3: Aluminum series with its major alloys elements (Downs 1993)

Alloy	Series No.	Example
Al	1XXX	1060
Co	2XXX	2219
Mn	3XXX	3004
Si	4XXX	4043
Mg	5XXX	5005
Mg/Si	6XXX	6061

Zn	7XXX	7005
Other	8XXX	8011

These eight major aluminum alloys series are generally divided into two groups heat treatable and non-heat treatable alloys as listed in Table 4.

Table 4: The major division for aluminum alloys (Downs 1993)

Heat Treatable	**NON Heat Treatable**
2000-Co	1000
6000-Mg-Si	3000
7000-Zn	4000
n/a	5000

2.6.2 Applications of Aluminum Alloys

Aluminum is a good conductor of heat and electricity, the conduction rate is three time faster than for steel and is second only for copper. This property is useful for the manufacturing of heat exchangers and many household cooking utensils. However, pure aluminum has a comparatively low melting point of 659 °C and must be alloyed for use in higher temperature applications. Two special properties make aluminum very valuable for electrical applications. Although, its conductivity rate is 62 % that of electrical grade copper, one pound of aluminum will go twice as far as copper when producing a conductor and it is less expensive. Additionally, a very large proportion of overhead, high voltages, power lines utilize aluminum rather than copper as the conductor on weight grounds. The relatively low strength of these grades requires that they be reinforced by including a galvanized or aluminum coated high tensile steel wire in each strand. For these reasons aluminum has replaced copper in many applications such as long-distance power lines, welding cables and

transforming wiring (Wrobel et al. 2014). Table 5 lists number of applications of some aluminum alloys.

Table 5: Aluminum series and its relative application (Farid et al. 2004)

Series No.	Application
1000	Electrical conductors
2000	Aircrafts
3000	Automobiles
4000	Welding filler metals
5000	railroad gondola
6000	Highway railing
7000	Armor plating

2.7 Welding of Titanium and Aluminum Alloys

Titanium and its alloys have different welding capability, in simple words they have moderate to excellent weldability. Figure 9 shows the various welding characterization of commercial pure titanium (CP Ti) and titanium alloys. In general, welding of titanium alloys is challenging due it its high sensitivity to oxidation during welding at 400 °C. However, this issue can be solved by providing argon gas shield.

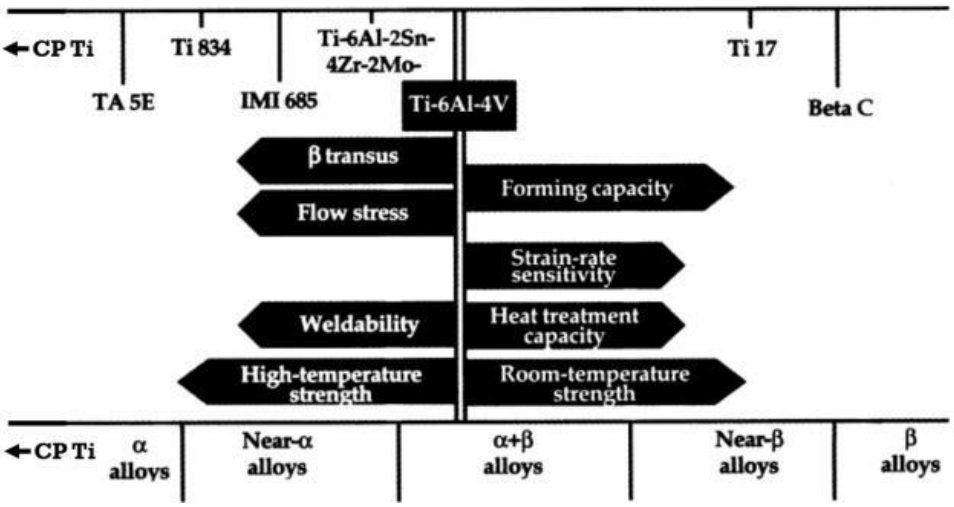

Figure 9:various welding characterization of CP titanium and its alloys (Mishra and DebRoy 2004).

Although, aluminum has highly desirable properties and numerous applications, it can be difficult to weld because of low melting point, high rate of thermal conductivity and surface oxides. Allowances must be made for heat buildup through the control of amperage settings and travel speed in order to prevent weld defects such as burn through as shown in Figure 10. In addition the oxide coating must thoroughly cleaned-off prior to welding since it easily combines with hydrogen in the air to produce moistures and resulting welding defects such as porosity as shown in Figure 11. During welding the solidifying aluminum can shrink as much as 60 % and is often the cause of cracking, and this defect can be prevented by preheating the joint, increasing the welding speed and cooling the weld pool.

Figure 10: Burn-through defect of aluminum (Kalpakjian et al. 2014)

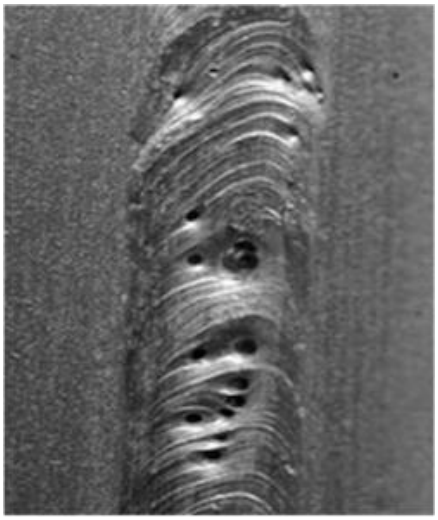

Figure 11: Porosity defect of aluminum (Kalpakjian et al. 2014)

Titanium and aluminum alloys are able to be welded by fusion welding techniques such as: plasma arc welding (PAW), gas metal arc welding (GMAW), gas tungsten arc welding (GTAW) or by solid-state welding process i.e. FSW and FSSW (Mishra and DebRoy. 2004).

2.7.1 Laser Beam Welding (LBW)

Laser Beam welding is known for high-power-density fusion welding process that creates high phase ratio welds with a moderately low heat-input compared with other arc-welding methods (Blackburn 2012). Liu et al. (2018) investigated the microstructure evolution of commercial pure titanium sheet during grain growth and recrystallization. The sheet has thickness 2.5 mm welded at laser power of 4 kW by using YLR 4000 fiber laser welding machine. Shielding gas of Argon was provided during welding to prevent contamination and oxidation on the sheet's surface. Specimens were cute from the sheet metal in order to apply a heat treatment on them at temperature of 625 to 700 °C and at holding time of 30 to 120 min in furnace. Results showed that base metal (BM) has smooth boundary and equiaxed shape, differs than fusion zone (FZ) and heat affected zone (HAZ) that contains serrated grain boundary with irregular shape. The high plastic strain which is expressed in terms of misorientation was also found. Figure 12 shows AS-welded at 4000KW/3m/min joint's macrostructure where the white dotted line separates BM from FZ and HAZ and also shows the grain boundary map of joint. However, it was not possible to distinguish the region of FZ from HAZ due to their similar orientation of gains.

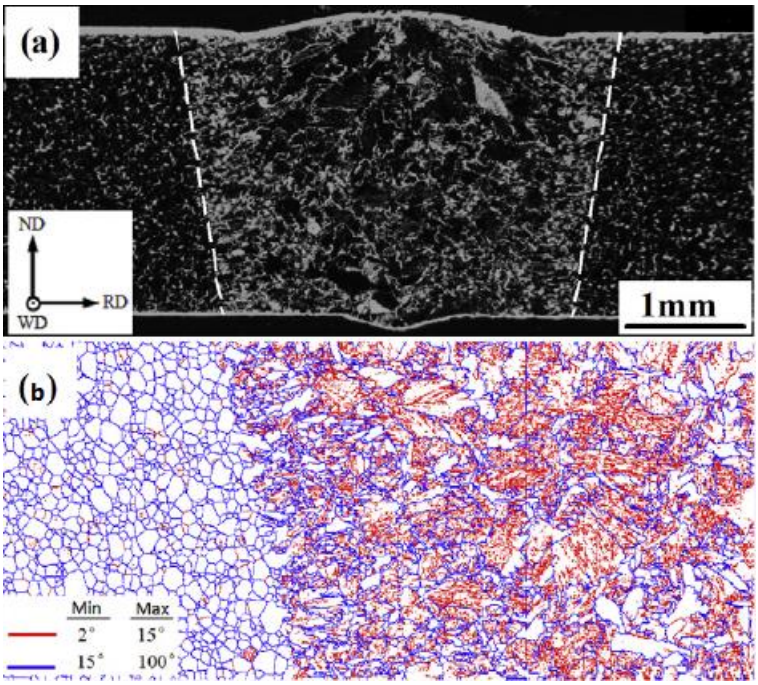

Figure 12: (a) macrostructure; (b) orientation map of grains (Liu et al. 2018)

2.7.2 Gas Metal Arc Welding (GMAW)

Early gas metal arc welding (GMAW) Showed limited ability to control heat input and to weld non-ferrous metals in a stable and efficient manner. However, (Zhang and Li 2001) have utilized conventional pulsed gas metal arc welding (P-GMAW) to join titanium alloy (ERTi-1) plate of 0.9mm in thickness, at pulse current output range of 5-450 A. during welding, Argon shielding gas of (99.999%) with flow rate of (20L/min) was provided. The equipment of the welding system was controlled by computer to generate a certain current in terms of waveform at constant arc length. The aim of experiment was to achieve the optimal welding parameters for the best stable and repeatable spray-transfer. Consequently, active control technology i.e. one drop per pulse (ODPP) mode was chosen to solve this problem. Furthermore, the electromagnetic force has increased and downward momentum was guaranteed, due to the proposed modified method that makes droplet starts to oscillate by first moving to the weld-pool. Nevertheless, (Cao et al. 2014) reported the properties and

microstructure of the titanium-copper lap-joint welded by the method of cold metal transfer (CMT) technology and developed GMAW process. The dissimilar lap joint consist of Cp Ti (TA2), copper (T2) and copper wire of (ERCuNiAl), and CMT method approved that it is a manner approach to join Ti-Cu dissimilar joint. Moreover, the tensile shear-strength was varied from 192.5 to 197.5 N/mm for the sample tested.

2.7.3 Gas Tungsten Arc Welding (GTAW)

This method is a fusion welding process that uses non-consumable tungsten head to join metals by heating-up workpiece to melting point. Nandagopal and Kailasanathan. (2014). have welded two dissimilar metals alloys of titanium (Ti-6Al-4V) and aluminum (7075) by conventional GTAW. Filler metal of aluminum (AA 4047) was used and welding parameters of (80-100 A), arc-voltage (14-18V) and welding speed (60-80 mm/min). The microstructural results revealed that joint is defect-free. In addition, the maximum tensile strength and hardness were 342.20 MPa and 183.10 Hv respectively.

2.7.4 Resistance Spot Welding (RSW)

Resistance Spot Welding (RSW) is designed to deliver low-voltage with high-current electrical pulse. The electrode is made of copper due to its low resistance to current flow which allows it to conduct electricity with ease. Aluminum alloys are very poor conductors of electricity and they will resist the weld current as it flows from the spot welder. The friction created by current forcing its way through the metal heats the weld area to over 1093 °C. The squeeze pressure from the weld electrodes compresses the molten area and fuses the two metals surfaces into one solid nugget by maintaining the squeeze pressure for short time after the weld current is shut off, which has known as Whole-time. Consequently, the molecules in the welded

material remain compressed as the weld cools. Spot-welding cycle is shown in Figure 13.

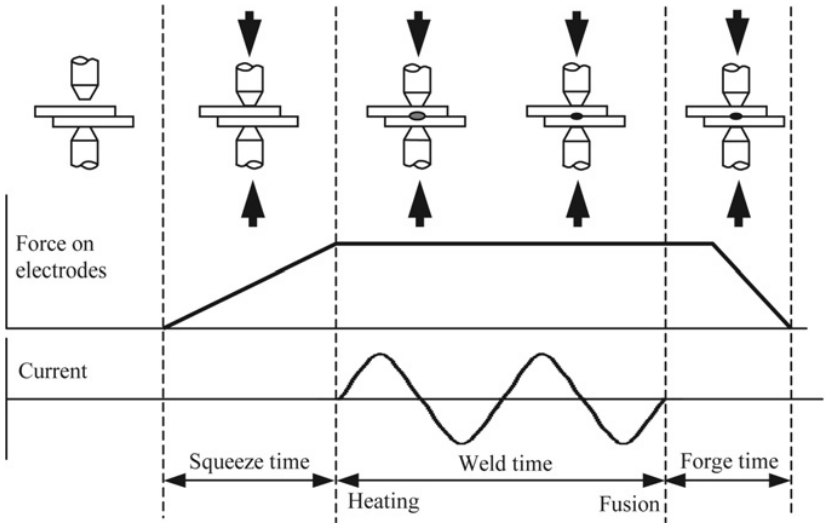

Figure 13: Spot-welding cycle (Nizamettin 2007)

RSW process was conducted by (Kahraman 2007) on commercially pure (CP) titanium sheets (ASTM Grade 2) at different welding parameters and under different welding environments. The welded joints were subjected to tensile-shearing tests in order to determine the strength of the welded zones. In addition, hardness and microstructural examinations were carried out in order to examine the influence of welding parameters on the welded joints. The results showed that increasing current time and electrode force increased the tensile shearing strength and the joints obtained under the argon atmosphere gave better shear tensile strength. Hardness measurement results indicated that welding nugget gave the highest hardness and the heat affected zone (HAZ) and the base metal followed this. The argon gas used during the welding process was seen to have no influence on the hardness values. Microstructural examinations revealed that the deformations took place in the welding zone during welding. Beam made of sheets has been welded utilizing RSW process by (Lacki and Derlatka 2017). The beam was made of two C-profiles of

aluminum alloy 6061-T6 sheets with the flanges stiffened by the titanium alloy grade 5 sheets with thickness of 0.8 mm. The flanges of the C-profiles were connected with the titanium alloy grade 5 sheets by RSW. Results show that the concentration of plastic strains occurs in the region of the RSW spot on the aluminum alloy sheet. However, Resistance Spot Welding has good mechanical quality.

2.8 FSSW Process Overview

Friction stir spot welding processes is an essential solid-state joining method by which high quality and high strength welds, in potentially difficult to weld alloys are possible. This technology is becoming vital choice for joining of light weight transportation structures such as; automotive, aerospace, light rails and marine applications. Moreover, it consider as a green process with no fumes or arc climate emitted nor welding wire consumed. As the increase in the demand of high efficient fuels in the automotive field; the FSW-FSSW are much desired to meet the costumers need in terms of designing light weight products combined with multi-material.

Also this technique has been proved that non-weldable series —e.g., (AA2xxx, AA6xxx, and AA7xxx) can be successfully welded in contrast to conventional welding techniques that causing liquation cracking in the HAZ Lancaster. (1999). FSSW process is capable to weld large number of high-temperature materials. However, since the focus of this research on FSSW of grade 5 titanium alloy "Ti-6Al-4V", FSSW is able to fabricate both butt and lap joints, in a varied range of material thicknesses and lengths.

2.8.1 Welding Parameters of FSSW

Several studies have been conducted to develop process parameters in achieving optimal joint strength and to provide recommendations of process guidelines. FSSW process has various welding parameters such as; rotation speed, dwell time, plunge depth and plunge rate .additionally, others as; different pin profiles are also have been investigated.

Henrich et al. (2009) studied the effects of rotational speed, plunge depth, plunge rate, and two tool geometries (not specified in details) on the tensile lap shear strength of 1.1mm 5754-O material using a design of experiment (DOE) approach. Highest failure load of 2.6 kN was obtained at lower rotational speed (1500 to 1750 rpm). Freeney et al. (2006) studied the effects of plunge rate, plunge depth, and rotational speed on the tensile shear failure load of 5052 H32 aluminum using a tapered-pin tool. They also found out that the lower rotational speed generated larger weld interface size which had higher weld strength. A failure load of about 4.2 kN was obtained with 1 mm thick samples and about 5 kN for 1.6 mm samples.

Chun et al. (2006) studied FSSW on 5052-H32 and 6111-T4, both in 1 mm thickness, and used a factorial experiment with the parameters of rotational speed (500 to 3,000 rpm), plunge depth (1.5 to 1.9 mm) and dwell time (0.5 to 2.5 sec). They concluded that the highest strength for 5052-H32 was achieved at 1,000 rpm; but 1,500 rpm for 6111-T4. FSSW tensile shear failure load for both materials was over 200% of the RSW specification from MIL-W-6858D standard. Tozaki et al. (2009) studied FSSW of dissimilar 2017-T6 to 5052 and used a threaded-pin, concave-shoulder tool. They found that lower rotational speed (1000 rpm) created

more extensive stir in the material, larger stir zone, and higher tensile shear strength, than higher rotational speed (2000 rpm).

However, recent researches on FSSW of titanium, aluminum and other alloys according to their material dimensions, tool material, tool geometry, welding parameters and failure forces have been summarized in Table 6.

Table 6: Recent researches on FSSW of various dissimilar alloys

Author	Materials	Materials dimensions (mm^3)	Tool material	Tool specifications (mm)	Pin profile	RPM	TPD (mm)	Dwell time (sec)	Max shear strength load (kN)	Fracture area	Remarks
Zhou et al. (2018)	2014-Al with hot dipped Ti-6Al-4V	80 × 35 × 3	GH4169	Pin ⌀ = 5 Shoulder ⌀ = 16 Pin L = 4	Circle threaded	900, 1200, 1500	0.3	15	14	SZ	• Increasing in the joining area due to Zn brazing region. • Increasing then decreasing of fracture loads with varying RPM.
Rojikin and Muhayat (2018)	AA 5052 with SS400	100 × 35 × 3 100 × 35 × 1.5	HSS	Pin-less Pin ⌀ = 12	cylindrical	1250, 1600, 2000	3.5	10	2.8	-	• Max shear strength obtained at 1600 RPM, but it decreased to 1.5 kN at 2000 RPM. • IMC increased with increase of RPM. • The largest Hook was detected at 2000 RPM.
Nader and Asgarani (2016)	Ti-6Al-4V	100 × 25 × 1.5	WC-Co	Pin ⌀ = 6 Pin ⌀ = 3 Shoulder ⌀ = 14 Pin L = 1.2	Conical (frustum)	800, 1000, 1250	-	7, 12	17.25	SZ,SZ,HAZ-SZ,HAZ,HAZ	• Peak temperature of SZ is higher than β-transus point. • Increasing in weld parameters results coarse grains. • SZ region showed the highest hardness value.
Patrick (2016)	AA1060 with C11000	600 × 120 × 3	Hardened H13	Pin ⌀ = 5 Shoulder ⌀ = 15 Pin L = 4	Flat pin and Shoulder and Conical pin and	800, 1200	0.5, 1	10	4.5 & 3.8	SZ	• 9.26 Max forge force, obtained with conical profile, 800rpm and 1 mm depth. • Extruded Cu produced

					concave shoulder						• interlock mode in SZ. • Presence of Cu ring (hook) in all spot welds.
Piccini and Svobod. (2014)	AA6063 with LCG-S	150 × 50 ×2 and 150 × 50 ×0.7	H13	Pin ⌀ = 3.5 Pin ⌀ = 3.7 Pin ⌀ = 38 Shoulder ⌀ = 11.7 a Pin L = 1.5 b Pin L = 1 c Pin L = 0.65	Conical	-	0.3 to 1.8	1	Max 4.7 with C tool	Interfacial	• Tools of shorter pins improve the forging and stirring of Al into S. • Short pins with increased TPD have improved EBL.
Venukumar et al. (2014)	AA 6061-T6	100 × 30 × 2	HCS-EN31	Pin ⌀ = 5 Shoulder ⌀ = 18	cylindrical	900, 1120, 1400, 1800	0.3,2.2 2	2	Max 9.5 by FSSW-FFP	Bonded regions	• Micrographs show different modes of failure in the conventional FSSW and FSSW-FFP weld samples. • Nugget pull-out and circumferential fracture mode were observed under different cycle loads.
Venukumar et al. (2013)	AA 6061-T6	100 × 30 × 2	HCS-EN31	Pin ⌀ = 5 Shoulder ⌀ = 18	cylindrical	900, 1120, 1400, 1800	-	-	Max 9.8, by FSSW	Bonded regions	• Grain refinements detected in SZ and TMAZ due to dynamic recrystallization. • Shear strength by FSSW-FFP at 1800 r/min and 9520 N and this value is 38.5% higher than that by conventional FSSW.

Tier et al. (2013)	AA 5042-O	140 × 60 × 1.5	-	Pin ⌀ = 5.2 Sleeve = 9 Shoulder ⌀ = 18	cylindrical	900, 1400, 1900	1.44, 1.55	-	6.3	Center and corner of weld	• Welds produced at higher tool rotational speed (1900 rpm) presented semi-elliptical SZ morphology, IB and streaks in the corner of the interface and shorter BLL. • Welds produced at a lower tool rotational speed (900 rpm) resulted in higher shear strength than welds produced at a higher rotational speed (1900 rpm).
Lee et al. (2011)	LCS with Al-Mg alloy	100 × 30 × 0.6	General steel	Pin ⌀ = 7 Shoulder ⌀ = 13 Pin L = 1	cylindrical	2500	0.2 to 0.5	2	3	-	• Excessive tool penetration beyond 0.4 mm resulted in welding defects. • Fe3Al and Fe4Al13 IMCs improved joint strength. • Increase in tool depth has increased shear strength.
Merzoug et al. (2010)	AA 6060-T5	163 × 64 × 2	X210 CR 12 steel	Pin ⌀ = 5 Shoulder ⌀ = 14 Pin L = 3.95	cylindrical	1000, 1400, 2000	-	10 to 50	Avg 5	-	• Weld quality increased with decrease in RPM. • Base metal microhardness range (80-100) HV and HV in SZ was 60 HV.

2.9 Gaps in Literature Review

After revising the literature review, it can be noticed a few gaps within authors researches:

- No sufficient studies about the effects of different welding parameters of Friction stir spot welding on titanium alloys.
- There are no adequate experimental studies on welding of dissimilar titanium alloys by FSSW process.
- In addition, change of microstructure and mechanical properties behavior of AA 6061 with Ti-6Al-4V alloys by FSSW is not yet reported.

Chapter 3

METHODOLOGY

3.1 Introduction

This chapter covers the research approach in terms of materials preparation, experimental setup, and investigations of mechanical behavior and microstructure of FSSWed joint. The flow chart below summarizes the experiment steps clearly in Figure 14.

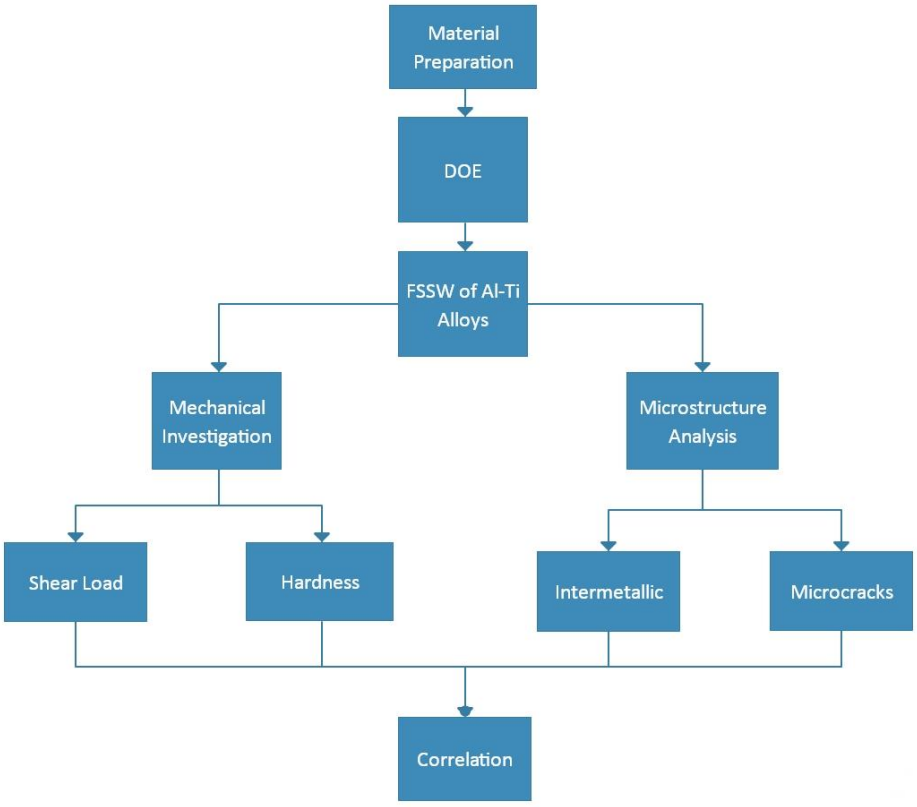

Figure 14: Research methodology process

3.2 Materials Preparation

The light weight metal of titanium Ti-6Al-4V and AA6061 plates alloy have a chemical composition as shown in Table 7 and Table 8 respectively were selected for friction stir sot welding process, as of their reliability and wide usage in multidisciplinary engineering industries such as aerospace and automobile. H13 steel tool was chosen to join the AA 6061 to Ti-6Al-4V plates, duo to its high melting point and density. The tool dimension are listed in Table. Argon gas was supplied during welding, in order to avoid titanium oxidation with due heat friction of the rotating tool.

Table 7: Ti-6Al-4V alloy chemical composition

Cr	Si	Fe	Cu	Nb	Ti	V	Al	Sn	Zr	Mo	C	Ni
0.0099	0.0222	0.112	<0.02	0.0386	90.00	4.22	5.48	0.0625	0.0028	0.005	0.369	<0.0010

Table 8: AA 6061 alloy chemical composition

Cr	Ti	Cu	Fe	Mg	Zn	Mn	Si	Others Each	Others Total	Al
0.04-0.35	0.15	0.15-0.40	0.7	0.8-1.2	0.25	0.15	0.40-0.80	0.05	0.15	Rem.

3.3 Experimental Setup

The grade-5 titanium alloy and AA 6061 plate with size of 100 × 35 × 4 mm^3 were selected for this experiment according to standard JIS Z 3136. Both of material were rinsed by worm water and then cleaned up by alcohol to insure removing contamination that can produce microscopic oxides. The aluminum plate was set on the top, due to its low melting point and ease of penetration comparing to titanium plate. The two plates were set-up into lap-joint configuration and then they have been fixed in the workpiece holder as illustrated in Figure 15. The workpiece was

positioned in the middle of the FSSW tool pin after adjusting the machine in the desired welding parameter.

Figure 15: Lap-joint configuration of dissmilare Al-Ti alloys

3.3.1 FSSW Tool

H13 steel alloy is a proper material to weld titanium alloy based on researches in the literature review, and it was chosen for its high mechanical efficiency at elevated temperatures, the tool was cut from 15 mm diameter rod and then it was machined by diamond wheel on the lathe machine into dimensions as listed in Table 9. The tool geometry is shown in Figure 16. Tool specification that is used for this experiment was adapted from (Hussain et al. 2018).

Table 9: H13 FSSW tool dimensions

Shoulder ϕ (mm)	Pin ϕ (mm)	Pin length (mm)
17	5	5.8

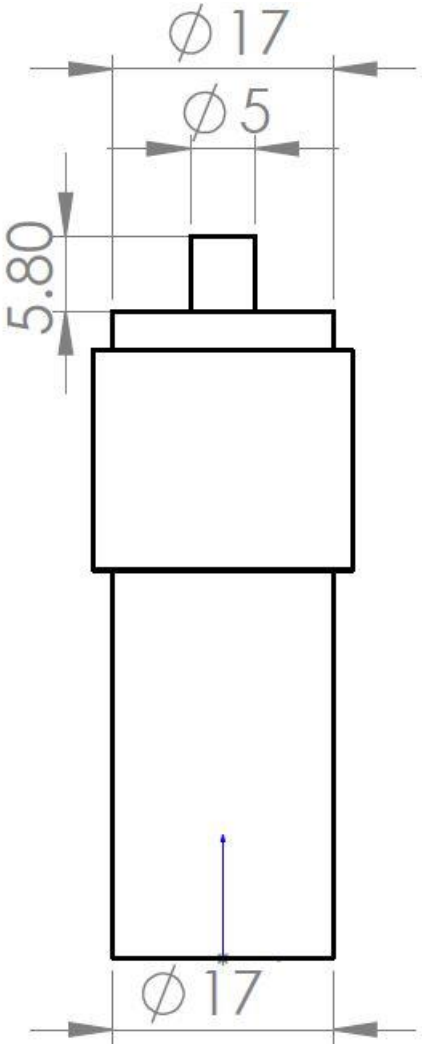

Figure 16: H13 FSSW tool

3.3.2 Welding Procedure

The semi-automated vertical milling machine as Shown in Figure 17, was modified to implement the FSSW process, thus the FSSW tool was installed vertically with respect to the workpiece's surface. Welding parameters were completely randomized using (Minitab 18.1) software. Full factorial design includes two quantitative levels (rotation speed & dwell Time) were selected for this experiment.

The tool was set on the joint surface after detecting the center point for penetration. After adjusting the desired speed the tool start to rotate and gradually penetrating the

upper surface until tool's shoulder and joint's surface meets. The shoulder has plunged approximately 0.3 mm into the upper plate and set for certain dwell time. As soon the dwell time ends, the tool is slowly lifted-up to avoid any distortion in the joint. After process is finished, the workpiece was left to cool down and to cohere tightly before removing it from the workpiece holder.

Figure 17: Vertical milling machine(vernier s8)

3.2.3 Design of Experiment (DOE)

Two-level, 2^k factorial design was selected to study the factors effect on the response (Shear load). Additionally, assuming that; factors are fixed, designs are completely randomized and usual normality assumption are satisfied. Two factors (A = rotation speed; B = Dwell time) with two levels "low" and "high" denoted by (-, +) were

selected respectively. 2^k Factorial design where, k = number of levels that indicates the total run, n = 4.

3.4 Mechanical Tests

In order to investigate the mechanical properties such as hardness and shear strength (failure load) of the FSSWed lap-joints, mechanical tests of Vickers and shear tensile test have been carried out.

3.4.1 Microhardness Test

The hardness values for welded metals for this experiment were measured by utilizing Vickers test of 0.5 HV, force 4.903 N and dwell time 10 sec. Several indents have been done along 10 mm distance within the cross-section of the welded workpiece as show in Figure 18 in order to investigate the hardness profiles pattern at the base metal and different weld regions. For each plate, the indentations were taken approximately 0.1 mm above and below the separation border line of joint. The test was done by utilizing the microhardness tester machine model (SHIMADZU HMV-FA Series) shown in Figure 19.

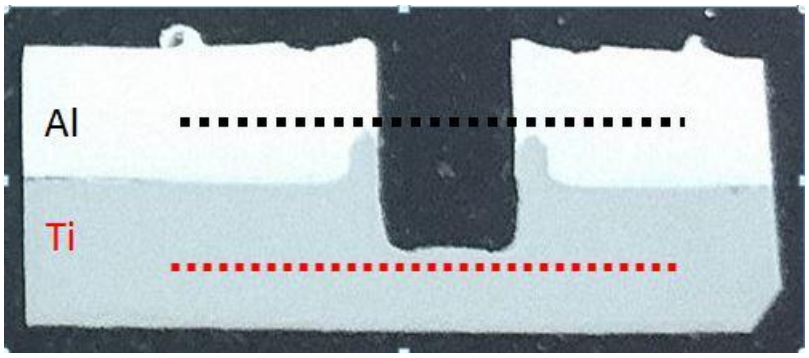

Figure 18: Microhardness indentations within joint cross-section

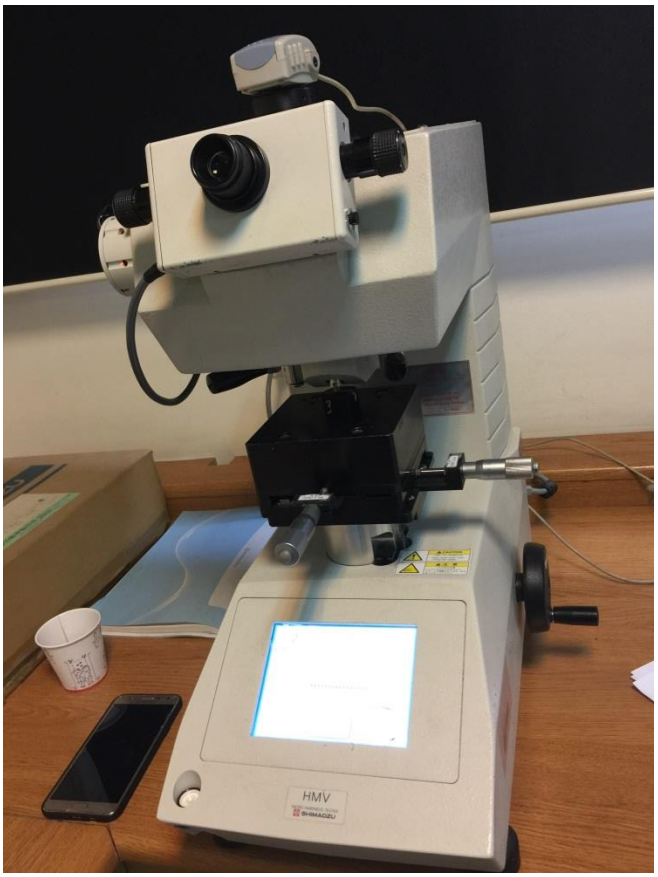

Figure 19: Microhardness test machine (SHIMADZU HMV-FA)

3.4.2 Shear Tensile Test

Specimens in lap-joint configuration are shown in Figure 20 have been sheared axially in order to investigate their failure loads and to observe their fracture modes. The shear strength load for the FSSWed plates was measured by using universal tensile test machine (INSTRON-5582). Specimens have been mounted between the machine's jaws as shown in Figure 21. The load rate was set at 3 mm/min for all runs.

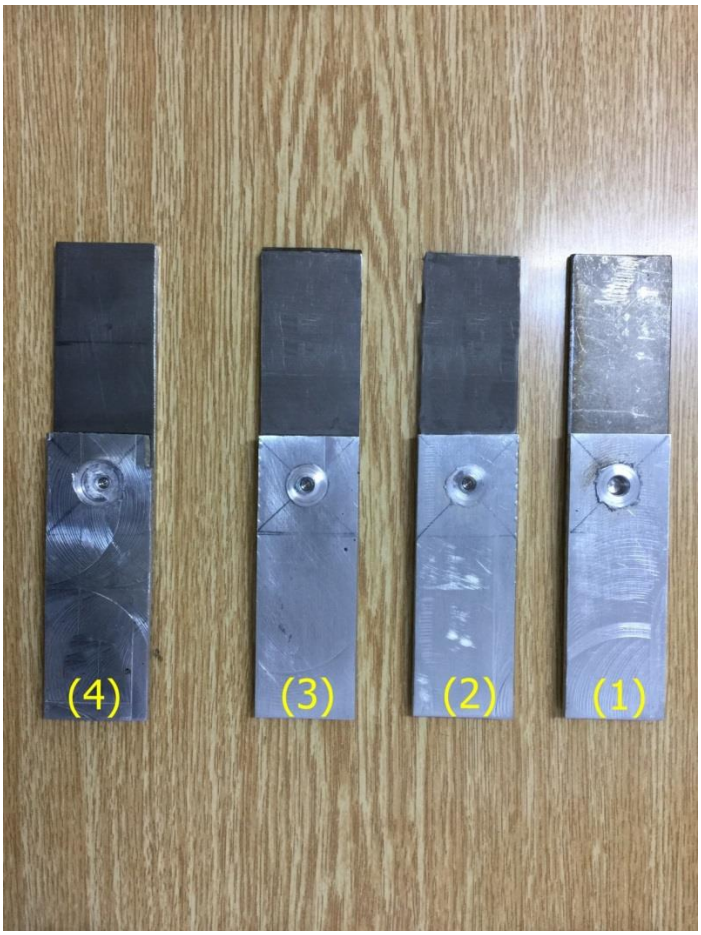

Figure 20: FSSWed Al-Ti lap-joint samples (1-4)

Figure 21: Universal tensile test machine (INSTRON-5582)

3.5 Metallographic Inspection

Different microstructures and grains orientations give different mechanical properties for metals, thus for this research scanning electron microscopy (SEM-EDS) analysis was carried out by using (JEOL JSM-6400) to detect any formed intermetallic compounds and to reveal the fine structure of different welded regions in FSSW joint. And also digital metallurgical microscope has been utilized in order to inspect the cross-sectional of FSSWed joints.

3.5.1 SEM-EDS Analysis

The welded samples for this experiment have been prepared carefully for the SEM-EDS analysis and the optical microscopic. All specimens are cut in the medal of their stir zones by using the precision cutting machine model (METACUT-251) that uses water coolant in order to avoid any heat input into the specimens. After the cutting process is done burrs and contaminations are removed from the surfaces. To facilitate the grinding and polishing processes; specimens are placed into the cylinder of the mounting press device with adding the Bakelite powder. The temperature is gradually raised in the cylinder chamber to 150 °C. Grinding and polishing processes have been carried out according to Voort. (1999) by, and solution of H_2O (95 ml) + HNO_3 (2.5 ml) + HCl (1.5 ml) + HF (1 ml) was used to etch the Al-Ti specimens. Polishing machine (MECAPOL-P230) and prepared specimens are shown in Figures 22 and 23 respectively. Figure 24 shows SEM-EDS machine used for this experiment.

Figure 22: MECAPOL-P230 polishing machine

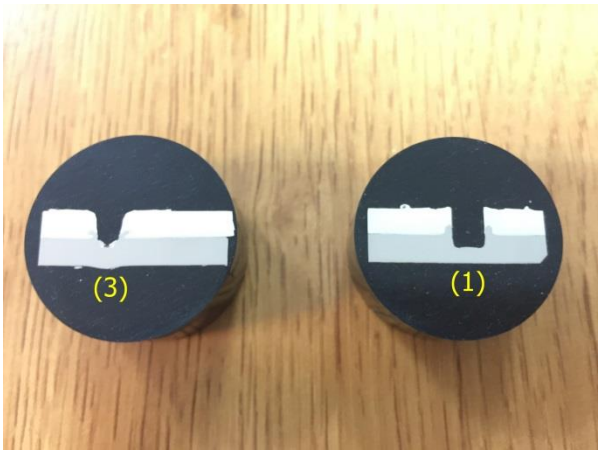

Figure 23: Al-Ti grinded and polished samples 1 and 3


Figure 24: SED-EDS machine (JEOL JSM-6400)

3.5.2 Metallurgical Microscope

A high magnification digital microscope (HUVITZ HDS-5800) as illustrated in Figure 25 with capability of 50x to 5800x magnification range was used to inspect the cross-section of the FSSWed specimens. The welded samples for this inspection process are prepared in the same manner for SEM-EDS analysis. Images of sectioned welded surfaces have been taken by utilizing 5x lens (50x magnification scale) in order to differentiate the various welded zones within the FSSWed joint.

Figure 25: Digital metallurgical microscope (HUVITZ HDS-5800)

Chapter 4

RESULTS AND DISCUSSION

4.1 Introduction

This chapter covers the results and discussion of the data obtained by conducting Friction Stir Spot Welding process of Al-Ti lap-joint using different welding parameters; rotation speed and dwell time. Furthermore, data obtained by DOE two-level factorial design were included. However, mechanical testing, such as the shear-tensile test and vickers microhardness test were covered. Metallographic inspection using the digital optical microscope and the scanning electron microscope (SEM) coupled with Energy Dispersive X-ray Spectroscopy (EDS) test were also conducted.

4.2 DOE

The two-level 2^k full factorial design was conducted with completely randomized data. Table 10 lists data obtained by FSSW process.

Table 10: Data obtained using two-level $\mathbf{2^k}$ full factorial design

StdOrder	RunOrder	A	B	RPM	Sec	Shear load
1	3	1	1	1400	15	2789.795
2	2	-1	1	1000	15	1787.523
3	4	-1	-1	1000	10	4224.338
4	1	1	-1	1400	10	1669.24

4.3 Microhardness Profiles within Al-Ti lap-joint

The microhardness profiles as illustrated in chapter 3 (see Figure 18) were done across the joint cross-section in order to observe the change in hardness values.

Figures 26 and 27 show the plotted microhardness profiles of Al-Ti sample 1 and 3 FSSWed at (10 sec, (1000 and 1400 rpm)) in terms of scatter straight lines respectively. It can be observed from Figures 26 and 27 that hardness profiles increase near SZ periphery while moving towards TMAZ for both of samples 1 and 3. This little increase is due to the plastic deformation caused by TMAZ (Mishra and Mahoney 2007). Next to the TMAZ denote the HAZ which ranges from point 2 to 5 symmetrically for both joints. HAZ hardness values reported higher values than TMAZ and this may due to increase in grain size of HAZ. Increase in rotation speed from 1000 to 1400 rpm drastically increased all hardness values of Ti alloys. Additionally, Hardness values of both Ti alloys in SZ were higher than HAZ measured hardness and these results were reported by (Piccini et al. 2015).

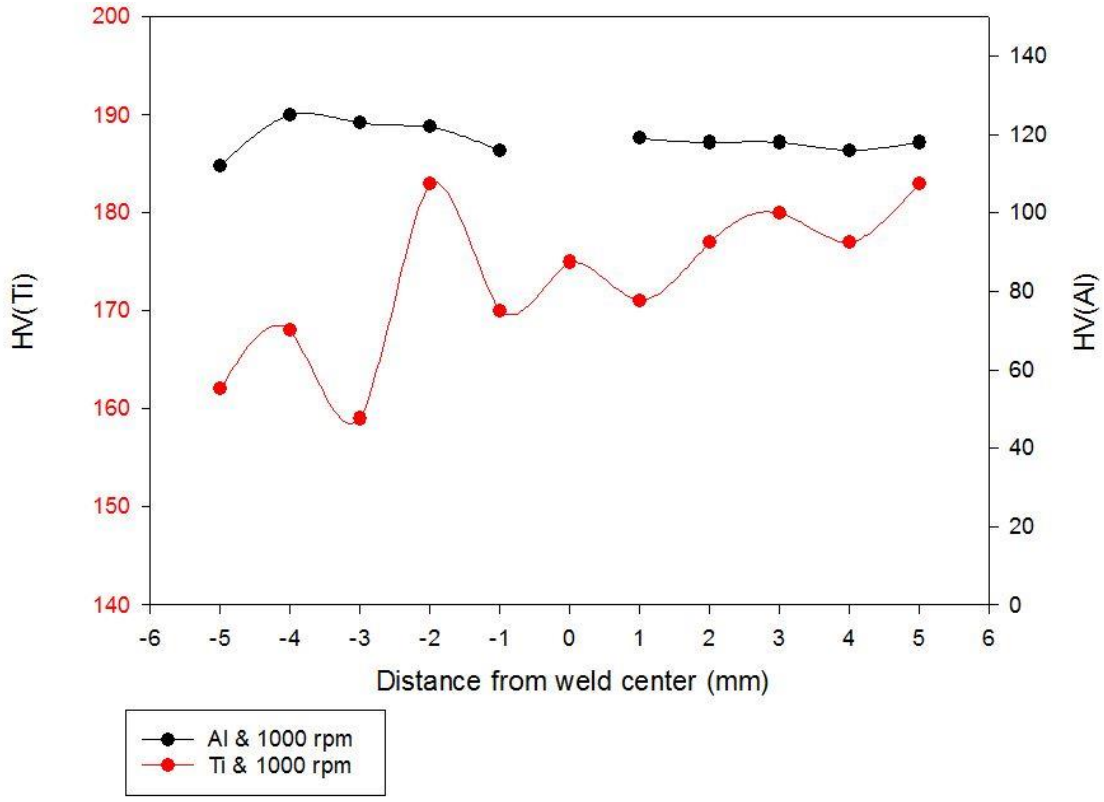

Figure 26: Microhardness profiles of sample 1

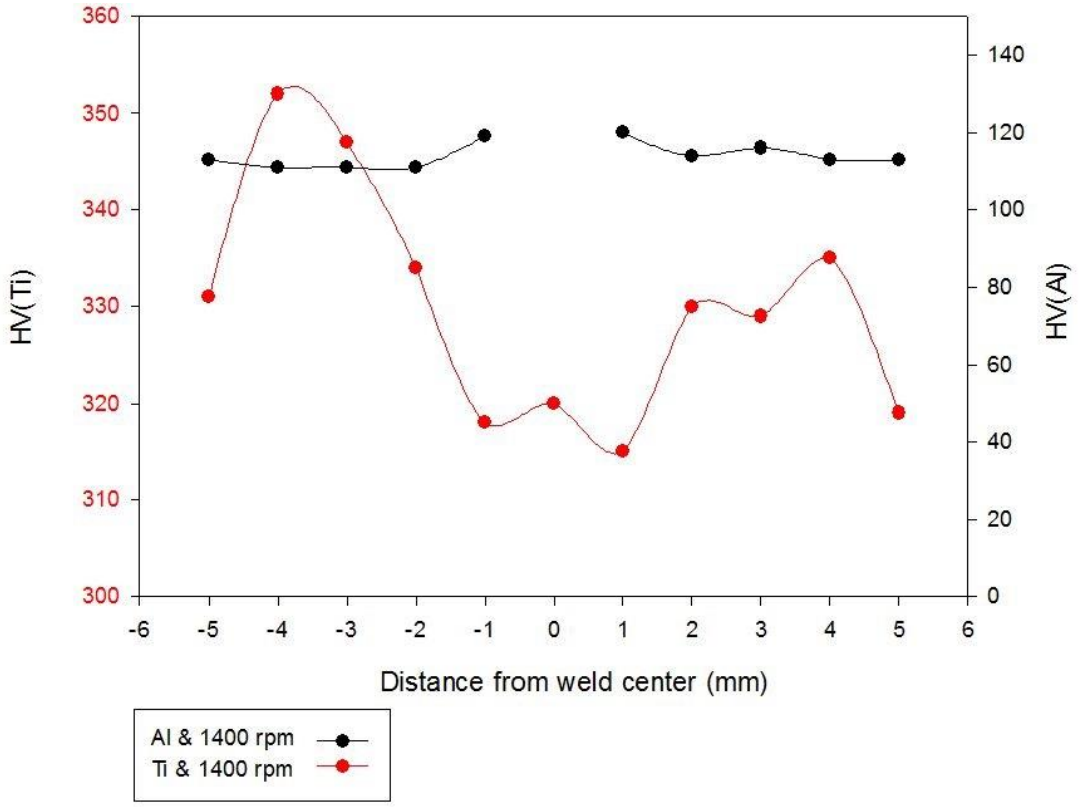

Figure 27: Microhardness profiles of sample 3

4.4 Shear Tensile Loads

Shear tensile test was conducted to determine the performance of FSSWed of aluminum and titanium joints under various welding parameters in terms of rotation speed and dwell time. The failure loads values of lap-joint samples are illustrated in Figure 28. The maximum failure load was 4.2 kN produced at 1000 rpm and 10 sec, which formed a larger SZ than higher rotational speed (1400 rpm), and these results were also reported by (Chang et al. 2006 , Tozaki et al. 2006). Decrease in failure load from 4.2 kN to 1.8 kN occurred after increasing in dwell to from 10 to15 sec. Failure load of 1.7 kN was obtained at 1400 rpm and 10 sec, thus this decrease is may occurred due to the formed micro-cracks within the SZ. However, the failure load has increased again from 1.7 to 2.5 kN when dwell is increased to 15 sec at 1400 rpm.

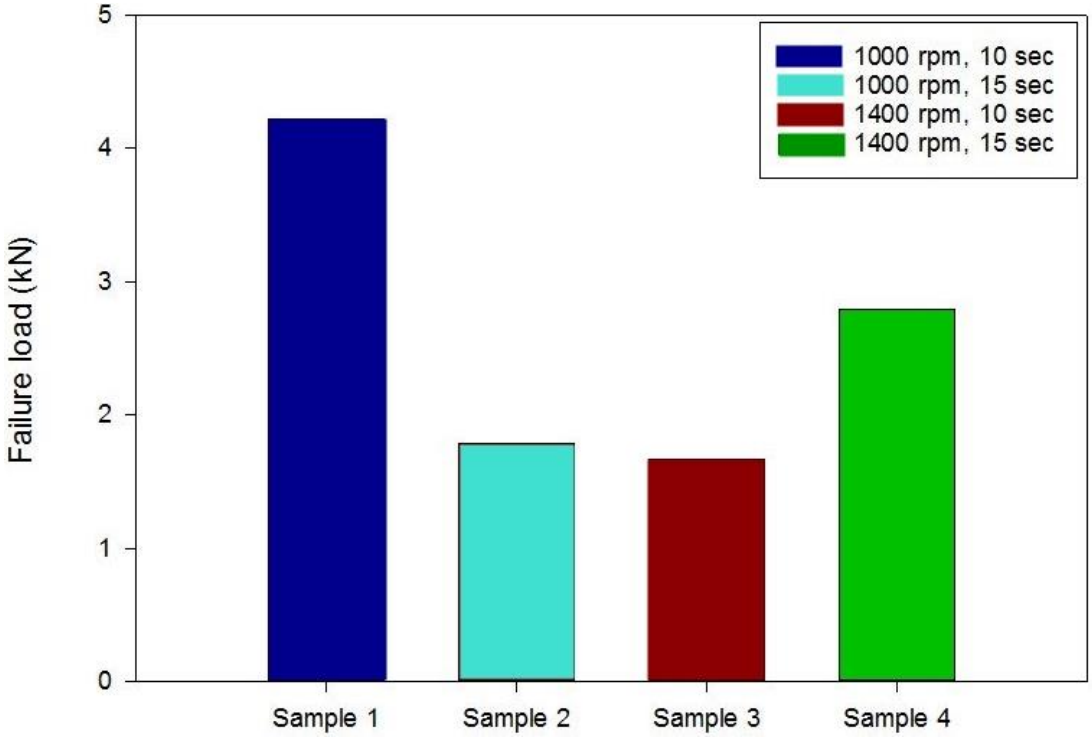

Figure 28: Failure loads values of samples 1-4, utilizing shear tensile test

4.5 SEM-EDS

Figure 29a shows the SEM microstructure image of SZ of sample1 joint. SEM-EDS analysis has been done within the SZ periphery at three yellow regions marked as (1, 2 and 3). IMC of $AlTi_3$ was detected at region 1 (partially bonded region; Hook) and at region 3 as shown in Figure 29d. Region 2 contains high amount of Al and few Zn elements. It can be observed from Figure 29a that both of left and right bonding regions are formed in vertical orientation, thus titanium has flowed into the aluminum material forming good bonded region with crack-free condition. Region 2 has initiated a long crack started from above the Hook region until it reached the upper surface of aluminum. This crack is initiated due to excessive tool lifting speed after the welding process is done. However, Figure 30a shows SZ of sample 3 and its regions (1, 2 and 3) at rotation speed of 1400 rpm. IMC of $AlTi_3$ was also detected by utilizing SEM-EDS analysis at regions 1 and 3 regions as illustrated in Figure 30a

& d. Region 2 illustrated in Figure 30c contains approx. 20 weight Conc% of Cr. This Cr element is formed from the melted H13 FSSW tool due to the excessive heat induced by high rotation speed. Furthermore, it can also be noticed that material residue of H13 tool was detected at the SZ root as shown in Figure 30a. Bonding regions of sample 3 are orientated with and angle of approx. 45°. Thus, titanium is flowed longer than sample 1 bonded region. However, microcracks are initiated within the bonded region, where it may be one of the reasons for the low failure load of sample 3.

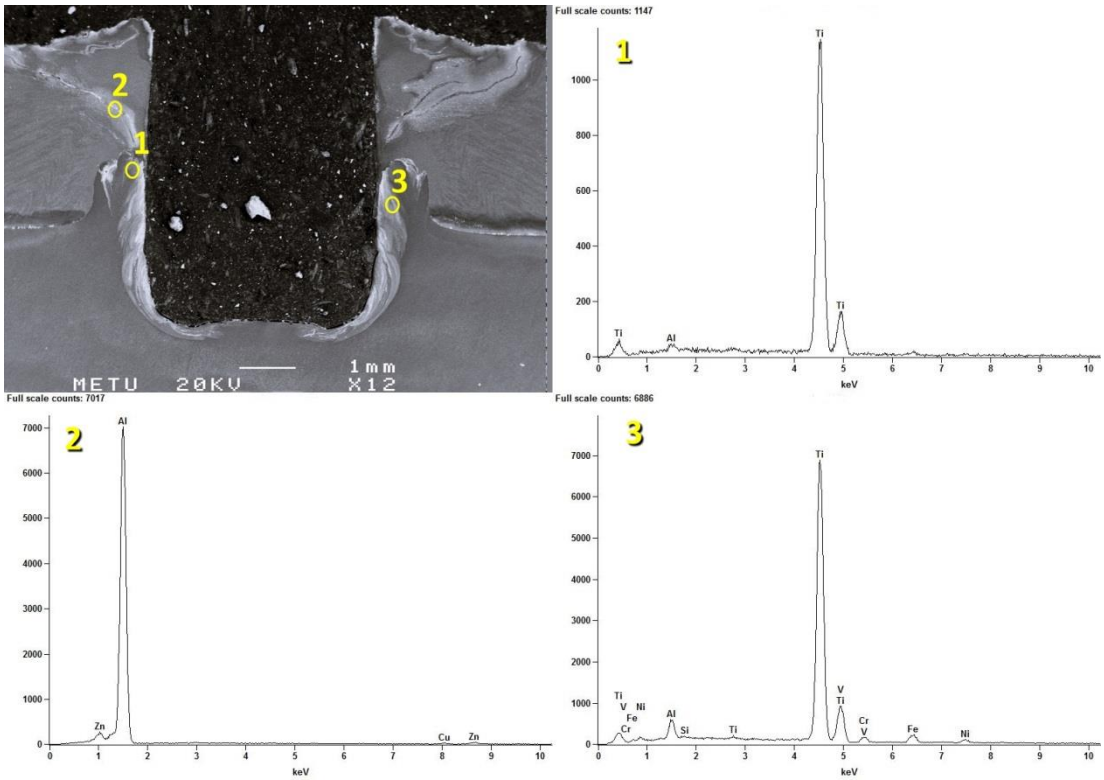

Figure 29: SEM image (a), EDS; (b) 1, (c) 2, (d) 3

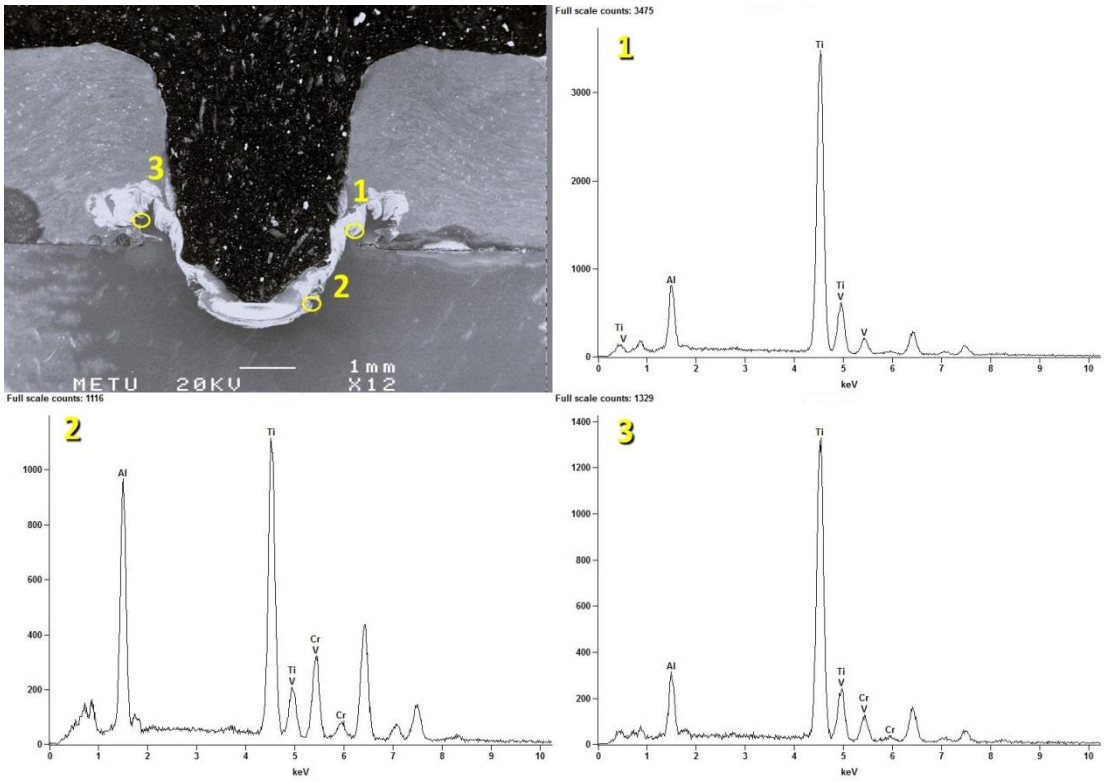

Figure 30: SEM image (a), EDS; (b) 1, (c) 2, (d) 3

4.6 Microstructure

The cross-section of FSSWed sample 1 produced at rotation speed of 1000 rpm and dwell time 10 sec is shown in Figure 31. It can be observed from this low magnification image that there is no H13 tool residue or microcracks into and around the SZ. The bonded width was found 1 mm, were titanium has penetrated vertically through the aluminum material due to the uniform mixing of the material by the FSSW tool. Figure 32 shows the cross-section of sample 3 FSSWed at 1400 rpm and 10 sec. The bonded width of sample 3 was larger than sample 1 by 40%, and thus shear failure load should be increased according to (Shen et al. 2014). However, this increase in the bonded area was non-effective due to the propagation of voids, microcracks near the Hook's periphery and because of the non-uniform material mixing, and thus these imperfections lead to decrease in the shear tensile load as reported by (Venukumar et al. 2013).

TMAZ and HAZ are illustrated in Figures 33 and 34 respectively. Figure 35 and 36 show the microstructure evolution of aluminum and titanium of sample 1 respectively. It can be observed that TMAZ (see Figure 35c) contains refined equiaxed grains and theses grains increase in size during moving towards HAZ (see Figure 35b & 36b).

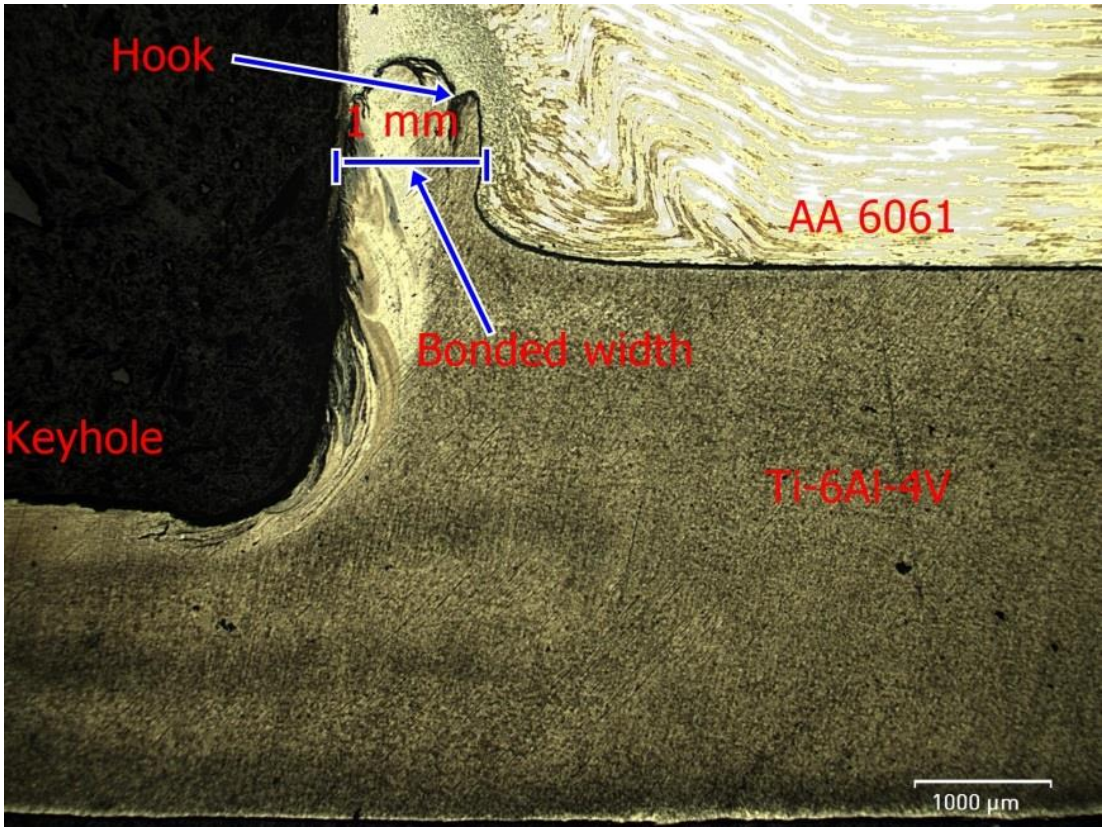

Figure 31: Cross-section of Sample 1. Dimensions lines have been measured via metallurgical microscope measurement.

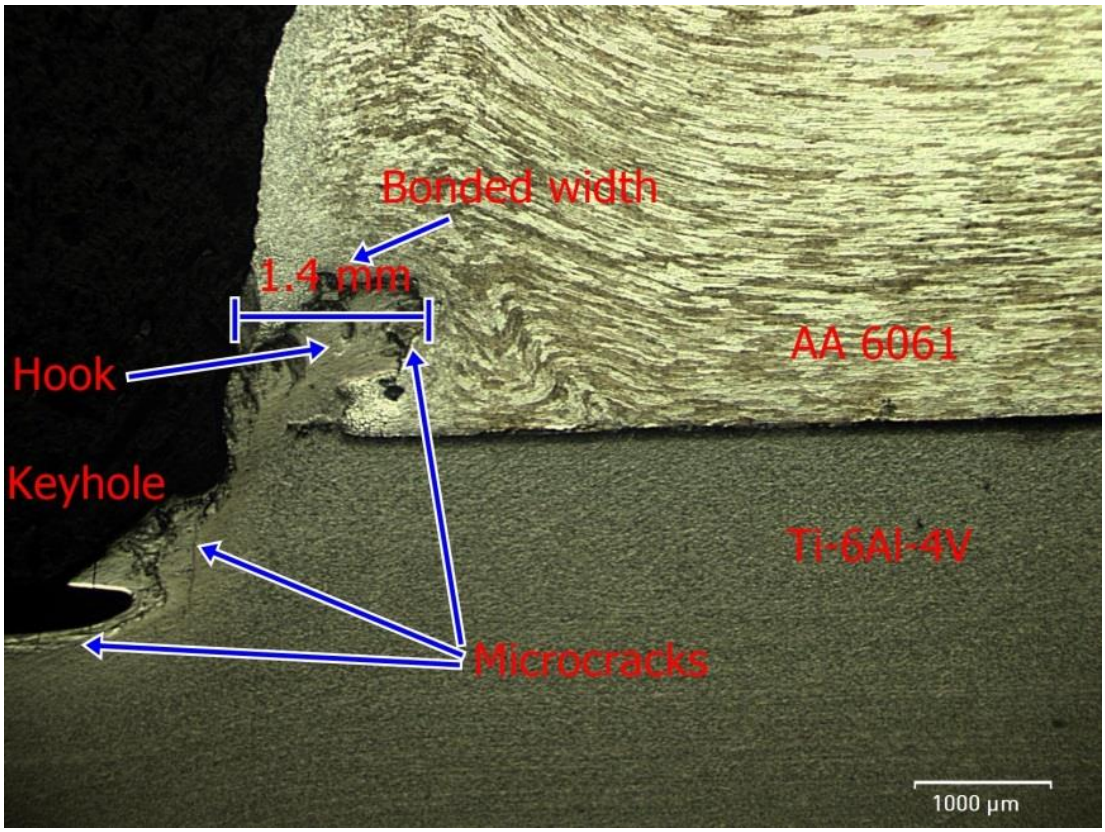

Figure 32: Cross-section of Sample 3. Dimensions lines have been measured via metallurgical microscope measurement.

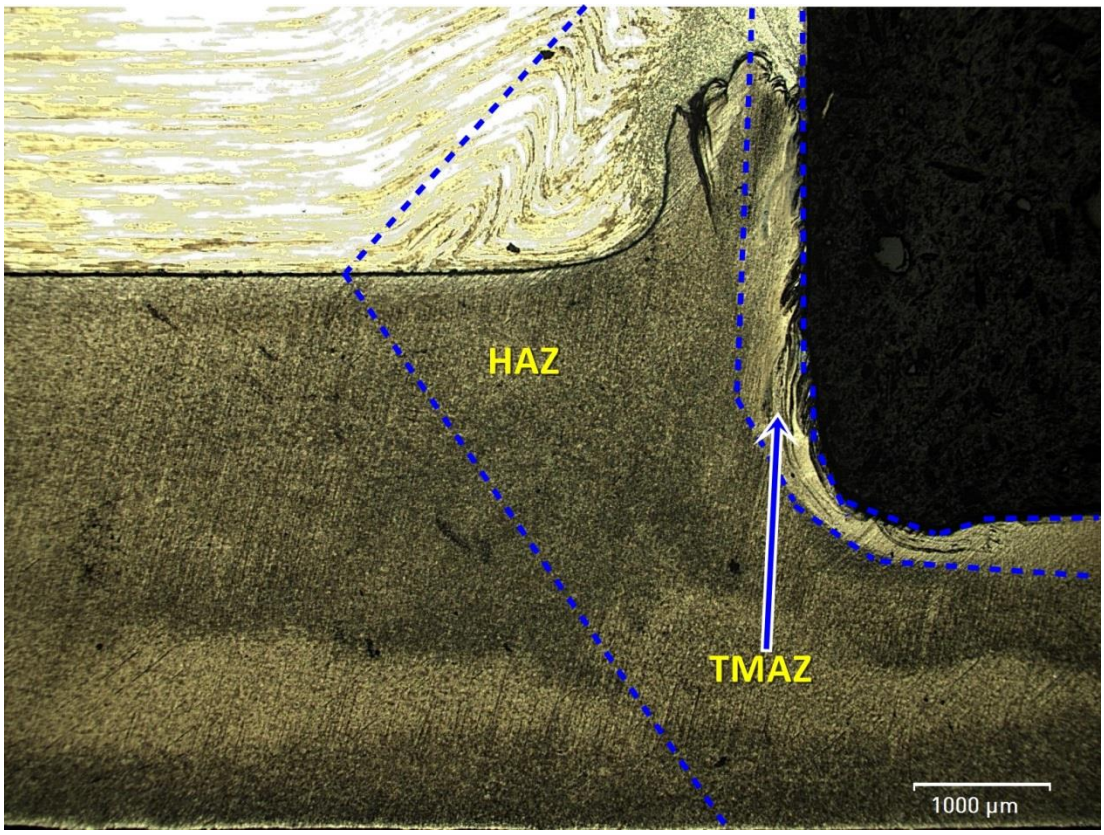

Figure 33: TMAZ and HAZ of FSSWed sample 1 cross-section. Photomicrograph was taken via metallurgical microscope

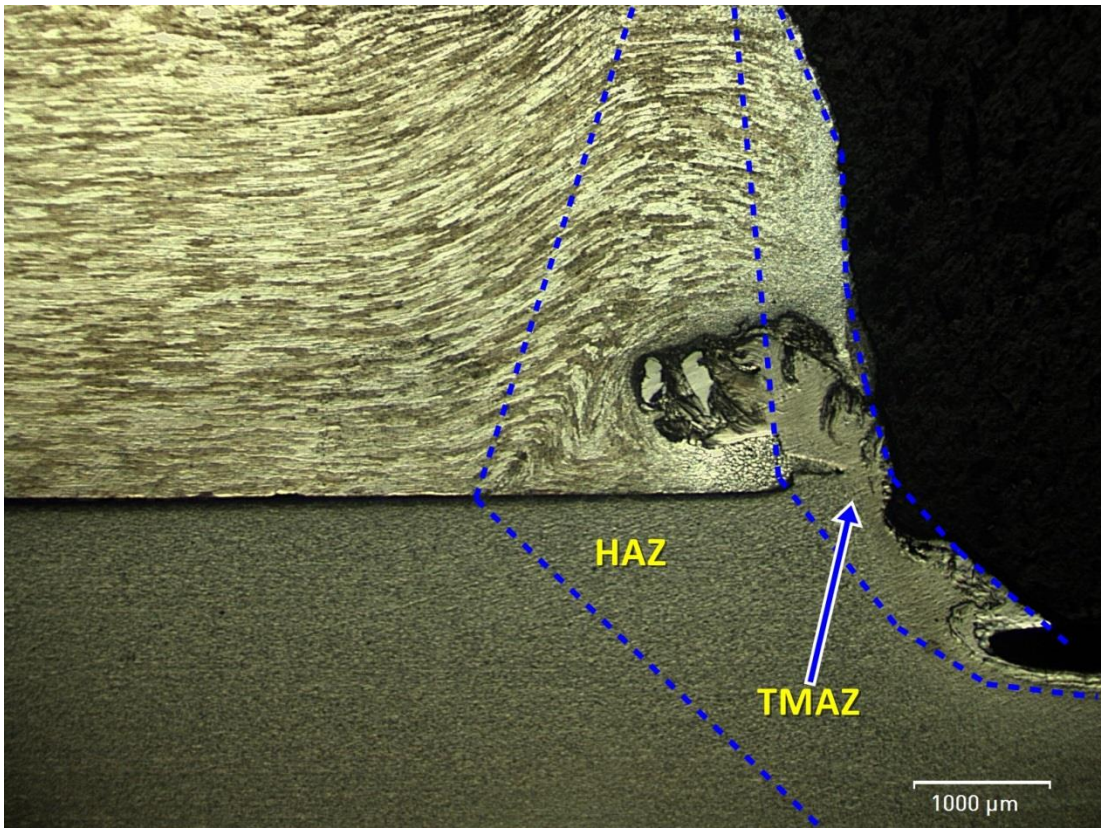

Figure 34**:** TMAZ and HAZ of FSSWed of sample 1 cross-section. Photomicrograph was taken via metallurgical microscope

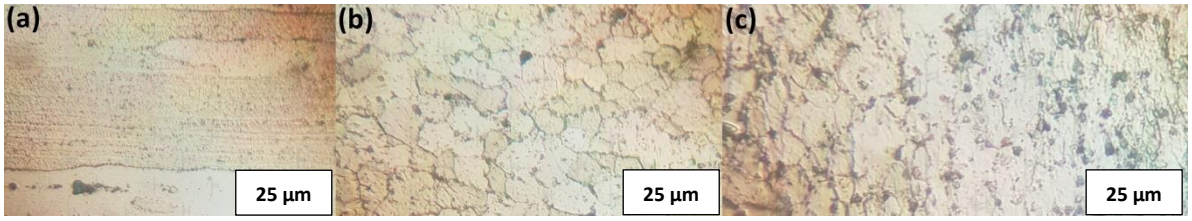

Figure 35: (a) Microstructure of Sample 1, Al cross-section (a) BM, (b) HAZ and (c) TMAZ. . Photomicrograph was taken via metallurgical microscope

Figure 36: (a) Microstructure of Sample 1, Ti cross-section (a) BM, (b) HAZ and (c) TMAZ. . Photomicrograph was taken via metallurgical microscope

Chapter 5

CONCLUSION

5.1 Introduction

The objective of this study was to join aluminum (AA 6061) and grade five titanium (Ti-6Al-4V) plates, utilizing friction stir spot welding process. This chapter concludes the effect of welding parameters; rotation speed and dwell time on the mechanical behavior and microstructure of the FSSWed lap-joint. Additionally, recommendations for future work to develop FSSW method are also presented.

5.2 Conclusion

In the present study, AA 6061 and Ti-6Al-4V dissimilar joint were successfully joined by friction stir spot welding process. The FSSWed joints were mechanically tested via shear tensile and Vickers hardness tests in order to investigate their mechanical behavior after processing. During applying shear tensile test on the lap-joints; the maximum failure load value was approx. 4.2 kN obtained at 1000 rpm and 10 sec dwell time. the value of failure load has decreased from 4.2 kN to 1.8 kN with increase in dwell time from 10 to 15 sec at 1000 rpm. The minimum load value was produced at 1400 rpm & 10 sec dwell time. Thus, this significant decreasing may be accrued due to the excessive heat-input that induced aluminum surface brittleness.

Based on shear results, Vickers test was applied on samples 1 & 3. Consequently, considerable changes have been observed where increasing in rotation speed from 1000 rpm to 1400 rpm has increased significantly microhardeness values within

HAZ and TAMZ of titanium. However this increase in tool speed did not affect HV values of aluminum considerably.

SEM-EDS analysis indicated the formation of intermetallic ($AlTi_3$) for samples 1 & 3 as discussed in chapter 4. This IMC has improved the shear load for sample 1. SEM image has shown the formation of larger SZ for sample 1 than sample 3 due to low rpm of FSSW tool. Solid imperfections (microcracks) were detected in TMAZ and Hook periphery within sample 3 by using digital optical microscope. Therefore, imperfections were formed due to excessive heat-input that lead to sharp decrease in the mechanical properties of sample 3.

5.3 Future Work

This thesis focused on some of the key issues in the understanding of the evolving properties of friction stir spot welding between aluminum and Titanium alloys. As a result of some of the findings, there are some additional areas that need to be addressed in more details in future research. These can be summarized in the following:

- Adding interlayer. i.e., Mg between Al-Ti lap-joint in order to increase the contact area and to compensate the solid imperfections at high rotation speed.
- Applying welding quality control technology. i.e., strain gage rosette (SGR) in order to investigate strain value near the SZ periphery.
- Temperature measurements need to be conducted to investigate the relation between temperature gradient and microstructure evolution of SZ, TMAZ and HAZ.
- Increasing the number of samples in order to conduct Artificial Neural Network (ANN) which generates a response surface model (RSM).

REFERENCES

Badarinarayan, H., Shi, Y., Li, X., & Okamoto, K. (2009). Effect of tool geometry on hook formation and static strength of friction stir spot welded aluminum 5754-O sheets. *International Journal of Machine Tools and Manufacture*, *49*(11), 814-823.

Badarinarayan, H., Yang, Q., & Zhu, S. (2009). Effect of tool geometry on static strength of friction stir spot-welded aluminum alloy. *International Journal of Machine Tools and Manufacture*, *49*(2), 142-148.

Baker, T. N. (2010). Laser surface modification of titanium alloys. In *Surface Engineering of Light Alloys* (pp. 398-443).

Belov, N. A., Eskin, D. G., & Aksenov, A. A. (2014). *Iron in aluminium alloys: impurity and alloying element*. CRC Press.

Blackburn, J. (2012). Laser welding of metals for aerospace and other applications. In *Welding and Joining of Aerospace Materials* (pp. 75-108).

Brick, R. M., & Phillips, A. L. (1949). Structure and properties of alloys.

Budai, D., Tisza, M., & Kovács, P. Z. (2017, February). Investigation of EN AW 5754 Aluminum Alloy's Formability at Elevated Temperatures. In *Material Science Forum* (Vol. 885, pp. 98-103).

Chang-Keun, C., Woong-Seong, C., & Hyeon-Jin, C. (2006). Study on Friction Spot Joining of Light Metal for Automotive. In 溶接学会全国大会講演概要 平成 18 年度春季全国大会 (pp. 72-72). 一般社団法人 溶接学会.

Chen, Y., Liu, C., & Liu, G. (2011). Study on the joining of titanium and aluminum dissimilar alloys by friction stir welding. *The Open Materials Science Journal*, *5*(1).

Danylenko, M. (2018). Aluminium alloys in aerospace. *Aluminium international today: the journal of aluminium production and processing*, *31*(4), 35.

Donachie, M. J. (2000). *Titanium: a technical guide*. ASM international.

Downs, A. J. (Ed.). (1993). *Chemistry of aluminium, gallium, indium and thallium*. Springer Science & Business Media.

Ducato, A., Fratini, L., La Cascia, M., & Mazzola, G. (2013, August). An automated visual inspection system for the classification of the phases of Ti-6Al-4V titanium alloy. In International Conference on Computer Analysis of Images and Patterns (pp. 362-369). Springer, Berlin, Heidelberg.

Farid, M. M., Khudhair, A. M., Razack, S. A. K., & Al-Hallaj, S. (2004). A review on phase change energy storage: materials and applications. *Energy conversion and management*, *45*(9-10), 1597-1615.

Freeney, T. A., Sharma, S. R., & Mishra, R. S. (2006). *Effect of welding parameters on properties of 5052 Al friction stir spot welds* (No. 2006-01-0969). SAE Technical Paper.

Fuji, A., Ameyama, K., Futamata, M., & Shimaki, Y. (1994). Effect of post-weld heat treatment on properties of commercially pure titanium/pure aluminium friction welds. Study of friction welding of titanium/aluminium (1st report).

Fujii, H., Takahashi, K., & Yamashita, Y. (2003). Application of titanium and its alloys for automobile parts. *Shinnittetsu giho*, 62-67.

Grimm, A., Schulze, S., Silva, A., Göbel, G., Standfuss, J., Brenner, B., ... & Füssel, U. (2015). Friction stir welding of light metals for industrial applications. *Materials Today: Proceedings*, *2*, S169-S178.

Grushko, O., Ovsyannikov, B., & Ovchinnokov, V. (2016). Aluminum-lithium Alloys: Process Metallurgy, Physical Metallurgy, and Welding. CRC press.

Haghshenas, M., & Gerlich, A. P. (2018). Joining of automotive sheet materials by friction-based welding methods: A review. *Engineering science and technology, an international journal*.

He, X., Gu, F., & Ball, A. (2014). A review of numerical analysis of friction stir welding. *Progress in Materials Science*, *65*, 1-66.

Inagaki, I., Takechi, T., Shirai, Y., & Ariyasu, N. (2014). Application and features of titanium for the aerospace industry. *Nippon steel & sumitomo metal technical report*, *106*, 22-27.

Islam, M. A., & Rahman, I. A Review of Properties of Advanced Aerospace Materials.

Kahraman, N. (2007). The influence of welding parameters on the joint strength of resistance spot-welded titanium sheets. *Materials & design*, *28*(2), 420-427.

Kalpakjian, S., Vijai Sekar, K. S., & Schmid, S. R. (2014). Manufacturing engineering and technology. Pearson.

Kar, A., Choudhury, S. K., Suwas, S., & Kailas, S. V. (2018). Effect of niobium interlayer in dissimilar friction stir welding of aluminum to titanium. *Materials Characterization*, *145*, 402-412.

Lacki, P., & Derlatka, A. (2017). Strength evaluation of beam made of the aluminum 6061-T6 and titanium grade 5 alloys sheets joined by RFSSW and RSW. *Composite Structures*, *159*, 491-497.Kahraman, N. (2007). The influence of welding parameters on the joint strength of resistance spot-welded titanium sheets. *Materials & design*, *28*(2), 420-427.

Lancaster, J. (1999). Metallurgy of Welding, Sexta Edicion ed., vol. Sexta Edicion, Abington.

Lee, C. Y., Choi, D. H., Yeon, Y. M., & Jung, S. B. (2009). Dissimilar friction stir spot welding of low carbon steel and Al–Mg alloy by formation of IMCs. *Science and Technology of Welding and Joining*, *14*(3), 216-220.

Lee, H. S., Yoon, J. H., Yoo, J. T., & No, K. (2016). Friction stir welding process of aluminum-lithium alloy 2195. *Procedia Engineering*, *149*, 62-66.

Liu, H., Shui, J., Cai, T., Chen, Q., Song, X. G., & Yang, G. J. (2018). Microstructural evolution and hardness response in the laser beam welded joints of pure titanium during recrystallization and grain growth. *Materials Characterization*, *145*, 87-95.

Lumley, R. (Ed.). (2010). Fundamentals of aluminium metallurgy: production, processing and applications. Elsevier.

Lütjering G., J.C. Williams, "Titanium", (Springer Verlag, Germany, 2007).

Mahoney, M. W., & Mishra, R. S. (2007). Friction stir welding and processing. ASM international.

Merzoug, M., Mazari, M., Berrahal, L., & Imad, A. (2010). Parametric studies of the process of friction spot stir welding of aluminium 6060-T5 alloys. Materials & Design, 31(6), 3023-3028.

Mironov, S., Sato, Y. S., & Kokawa, H. (2018). Friction-stir welding and processing of Ti-6Al-4V titanium alloy: A review. *Journal of Materials Science & Technology*, *34*(1), 58-72.

Mishra, S., & DebRoy, T. (2004). Measurements and Monte Carlo simulation of grain growth in the heat-affected zone of Ti–6Al–4V welds. *Acta Materialia*, *52*(5), 1183-1192.

Mubiayi, M. P. (2015). *Characterisation of the evolving properties of friction stir spot aluminium and copper welds*(Doctoral dissertation, University of Johannesburg).

Mubiayi, M. P., Akinlabi, E. T., & Makhatha, M. E. Current Trends in Friction Stir Welding (FSW) and Friction Stir Spot Welding (FSSW).

Mvola, B., Kah, P., & Martikainen, J. (2014). Welding of dissimilar non-ferrous metals by GMAW processes. *International Journal of Mechanical and Materials Engineering*, *9*(1), 21.

Nader, S., Kasiri-Asgarani, M., Amini, K., & Shamanian, M. (2016). Effect of Welding Parameters on Microstructure and Mechanical Properties of Friction Stir Spot Welded of Titanium Alloy TiAl6V4. *International Journal of Advanced Design & Manufacturing Technology*, *9*(2).

Padmanabhan, R., Oliveira, M. C., & Menezes, L. F. (2011). Lightweight metal alloy tailor welded blanks. In *Tailor Welded Blanks for Advanced Manufacturing* (pp. 97-117).

Pan, T. Y. (2007). *Friction Stir Spot Welding (FSSW)-A Literature Review* (No. 2007-01-1702). SAE Technical Paper.

Pasha, A., Reddy, R., Laxminarayana, P., & Khan, I. A. (2014). influence of process and tool parameters on friction stir welding–OVER VIEW. *Int J App Eng Technol*, *4*(3), 54-69.

Pearson, W. B. (2013). *A handbook of lattice spacings and structures of metals and alloys: International series of monographs on metal physics and physical metallurgy* (Vol. 4). Elsevier.

Piccini, J. M., & Svoboda, H. G. (2015). Effect of pin length on Friction Stir Spot Welding (FSSW) of dissimilar Aluminum-Steel joints. *Procedia Materials Science*, *9*, 504-513.

Rambabu, P. P. N. K. V., Prasad, N. E., Kutumbarao, V. V., & Wanhill, R. J. H. (2017). Aluminium alloys for aerospace applications. In *Aerospace Materials and Material Technologies* (pp. 29-52). Springer, Singapore.

Ramirez, A. J., & Juhas, M. C. (2003). Microstructural evolution in Ti-6Al-4V friction stir welds. In *Materials Science Forum* (Vol. 426, pp. 2999-3004). Trans

Tech Publications Ltd., Zurich-Uetikon, Switzerland.Yuan, W. (2008). Friction stir spot welding of aluminum alloys.

Rojikin, S., & Muhayat, N. (2018, September). Effect of rotation speed on mechanical properties and microstructure of friction stir spot welding (FSSW) Al 5052-Steel SS400. In IOP Conference Series: Materials Science and Engineering (Vol. 420, No. 1, p. 012023). IOP Publishing.

Shen, J., Wen, L., Luo, X., Xu, N., Wang, D., & Liu, M. (2014). Development of novel heating tool friction stir spot welding (HT-FSSW) for AZ31 magnesium alloy. Science and Technology of Welding and Joining, 19(5), 369-375.

Shouzheng, W., Yajiang, L., Juan, W., & Kun, L. (2014). Research on cracking initiation and propagation near Ti/Al interface during TIG welding of titanium to aluminium. *Kovove Mater*, *52*, 85-91.

Tier, M. D., Rosendo, T. S., Dos Santos, J. F., Huber, N., Mazzaferro, J. A., Mazzaferro, C. P., & Strohaecker, T. R. (2013). The influence of refill FSSW parameters on the microstructure and shear strength of 5042 aluminium welds. *Journal of materials processing technology*, *213*(6), 997-1005.

Tisza, M., & Czinege, I. (2018). Comparative study of the application of steels and aluminium in lightweight production of automotive parts. *International Journal of Lightweight Materials and Manufacture*, *1*(4), 229-238.

Tozaki, Y., Uematsu, Y., & Tokaji, K. (2006, October). Effect of welding condition on tensile strength of dissimilar FS Spot welds between different Al alloys. In Proceedings of the 6th International Symposium on Friction Stir Welding, Saint-Sauveur, Nr Montreal, Canada, October (pp. 10-13).

Vander Voort, G. (1999). Metallographic preparation of titanium and its alloys. Buehler Tech-Notes, 3(3).

Venukumar, S., Muthukumaran, S., Yalagi, S. G., & Kailas, S. V. (2014). Failure modes and fatigue behavior of conventional and refilled friction stir spot welds in AA 6061-T6 sheets. *International Journal of Fatigue*, *61*, 93-100.

Venukumar, S., Yalagi, S., & Muthukumaran, S. (2013). Comparison of microstructure and mechanical properties of conventional and refilled friction stir spot welds in AA 6061-T6 using filler plate. *Transactions of Nonferrous Metals Society of China*, *23*(10), 2833-2842.

Wang, G., Zhao, Y., & Hao, Y. (2018). Friction stir welding of high-strength aerospace aluminum alloy and application in rocket tank manufacturing. *Journal of Materials Science & Technology*, *34*(1), 73-91.

Wang, G., Zhao, Y., & Hao, Y. (2018). Friction stir welding of high-strength aerospace aluminum alloy and application in rocket tank manufacturing. *Journal of Materials Science & Technology*, *34*(1), 73-91.

Wang, K. (1996). The use of titanium for medical applications in the USA. *Materials Science and Engineering: A*, *213*(1-2), 134-137.

Wrobel, R., Salt, D., Simpson, N., & Mellor, P. H. (2014). Comparative study of copper and aluminium conductors-future cost effective PM machines.

Yamaguchi, J. (2004). Toyota Prius: AEI best engineered vehicle 2004. *Automotive Engineering International*, 42-44.

Yang, X. W., Fu, T., & Li, W. Y. (2014). Friction stir spot welding: a review on joint macro-and microstructure, property, and process modelling. *Advances in Materials Science and Engineering*, *2014*.

Zhang, Y. M., & Li, P. J. (2001). Modified active control of metal transfer and pulsed GMAW of titanium. *Analysis*, *17*, 19.

Zhou, X., Chen, Y., Li, S., Huang, Y., Hao, K., & Peng, P. (2018). Friction Stir Spot Welding-Brazing of Al and Hot-Dip Aluminized Ti Alloy with Zn Interlayer. *Metals*, *8*(11), 922.